수의학 석사 학위논문

Studies of Improved Metabolic Phenotype on Sema4D Knockout Mouse

Sema4D Knockout Mouse의

대사 표현형 연구

2020년 **08**월

서울대학교 대학원

수의학과 수의생명과학 전공

김 경 은

A Dissertation for the Degree of Master of Science

Studies of Improved Metabolic Phenotype on Sema4D Knockout Mouse

August 2020

Kyoungeun Kim

Supervisor: Pro. Je Kyung Seong, D.V.M., Ph.D.

Department of Veterinary Medicine

College of Veterinary Medicine

Developmental Biology and Genomics

The Graduate School of Seoul National University

Studies of Improved Metabolic Phenotype on Sema4D Knockout Mouse

지도교수 성 제 경

이 논문을 수의학석사 학위논문으로 제출함

2020년 5월

서울대학교 대학원

수의학과 수의생명과학 전공

김 경 은

김경은의 수의학석사 학위논문을 인준함

2020년 7월

위 원 장 윤 여 성 (인)

부 위 원 장 성 제 경 (인)

위 원 백 승 준 (인)

Abstract

Studies of Improved Metabolic Phenotype on Sema4D Knockout Mouse

Kyoungeun Kim
College of Veterinary Medicine
Developmental Biology and Genomics
The Graduate School
Seoul National University

Semaphorin 4D is a group 4 Semaphorin that is related to B cell development and class switching. Effects of B cell differentiation in adipose tissue inflammation and glucose homeostasis have not been clearly understood. Obesity is known to induce B cell activation and pathogenic antibodies from activated B cells accelerate adipose tissue inflammation and insulin resistance. Here, we report that Semaphorin 4D deficiency improved glucose dysfunction in high-fat diet-induced obese mice. Inflammation was decreased in high-fat diet fed Semaphorin 4D knockout mice and the production of class

switched immunoglobulin IgG2c was also reduced. Consistently, adipose tissue inflammation was also alleviated and the sizes of adipocytes and the masses of adipose tissues were reduced as well, which resulted in decreased body weight. These were confirmed by the decreased expression of genes related with lipid metabolism and adipogenesis and improved respiratory exchange ratio. In summary, these data indicate Semaphorin 4D as a crucial regulator in metabolic homeostasis and glucose metabolism via B cell development.

Keywords: Semaphorin 4D, obesity, adipose tissue inflammation, B lymphocytes, glucose homeostasis, mouse

Student Number: 2018-22461

List of Abbreviation

Abhd5	Abhydrolase domain containing 5
AUC	Area under the curve
CCL2	Chemokine (C-C motif) ligand 2
CD	Cluster of differentiation
C/EBPα	CCAAT/enhancer binding protein alpha
Dgat2	Diacylglycerol O-acyltransferase 2
Hsl	Hormone-sensitive lipase
DIO	Diet induced obesity
eWAT	Epididymal white adipose tissue
HFD	High fat diet
IFN-γ	Interferon gamma
Ig	Immunoglobulin
IKKβ	I-kappa B kinase
IL-1β	Interleukin 1 beta
KO	Knock out
NCD	Normal chow diet
NF-κB	Nuclear factor kappa-light-chain-enhancer of activated B cells
Plin1	Perilipin1
Plin2	Perilipin2

PPARγ	Peroxisome proliferator-activated receptor gamma
RER	Respiratory exchange ratio
Sema4D	Semaphorin 4D
SHP-1	Src homology region 2 domain-containing phosphatase-1
T2DM	Type 2 diabetes mellitus
TNF-α	Tumor necrosis factor alpha
WT	Wild type

Contents

List of Figures

List of Tables

Introduction

Semaphorin is a large family of proteins divided into 8 different subclasses. All the semaphorin subclasses carry Sema domain which is about 500 amino acids. [1] [3] [12] [20] [23] Since Sema domain is phylogenetically well conserved, classes 3 to 7 are found in vertebrates while 1 and 2 are in invertebrate species. [1] [21] [32] These semaphorins are first known as axonal guidance factors, related to neuronal development. [1] [3] In addition to axonal pathfinding, semaphorins play various roles in organogenesis, vascularization, angiogenesis, apoptosis, neoplastic transformation, progression of cancer, osteogenesis, reproduction, respiratory, and musculoskeletal systems. [1] [12] [20] [23] [24] [30] However, some semaphorins have been emerging to have roles in immune regulation, called ‘immune semaphorins’. Semaphorin 3A, 3E, 4A, 6D, and 7A have been discovered since Semaphorin 4D (Sema4D, also known as CD100) was known as the first immune semaphorin. [1] [20] [21] [22] [23] [30] [39] Sema4D is expressed on various immune cells like resting T cells and antigen-presenting cells but largely expressed on T cells and increased after cellular activation. [1] [3] [20] [21] [23] [24] [39] Sema4D acts as an antigen on T cell surface and interacts with CD72 which is dominantly expressed on B cells. [1] [3] [5] [12] If Sema4D interacts with CD72, B cell responses are affected by

intracellular signaling of CD72. CD72 has immunoreceptor tyrosine-based inhibitory motifs (ITIM) on its cytoplasmic region and SHP-1, tyrosine phosphatase, is normally phosphorylated and docked on the motifs. Phosphorylated SHP-1 inhibits the signal through B cell receptor or CD40 and CD72 activation by Sema4D dephosphorylate the SHP-1, resulting in enhanced B cell responses (Fig. 1). Furthermore, Sema4D is known to induce proteolysis of CD23 from B cell surface. When CD23 is shed from B cell surface, immunoglobulin class switching to IgG or IgE is increased. Therefore, Sema4D modulates CD72 to enhance B cell activation, differentiation and eventually production of class switched immunoglobulins. [1] [3] [12] [20] [23] [39]

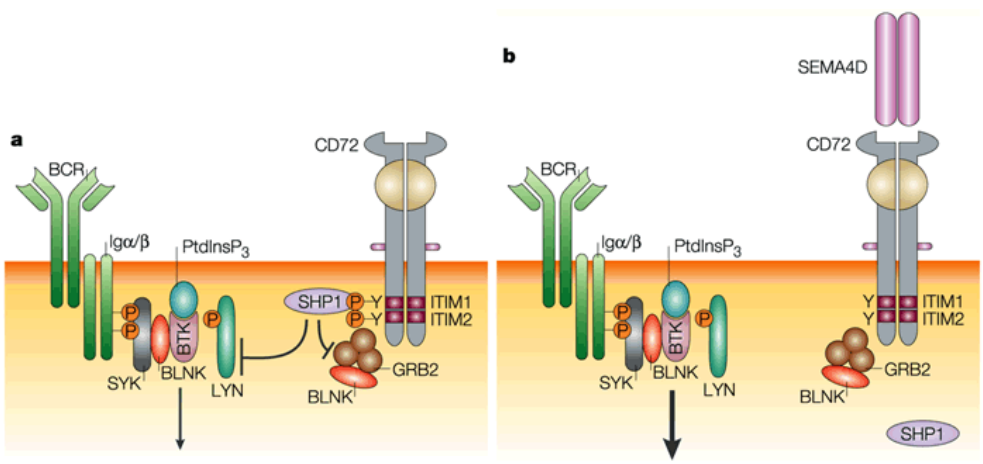

Nature Reviews | Immunology

Figure 1. Semaphorin 4D and CD72 interaction and B cell receptor signal. (Kikutani, H. & Kumanogoh, A., Nat. Rev. Immunol., 2003)

B cells, which is the target of Sema4D, were the most recent immune cells to be studied in metabolism. However, B cells recently have been spotlighted to be linked with modulating glucose homeostasis as inhibition of B cells or B null mice lacking Igh6 dramatically relieved insulin resistance. High fat diet induces production of class switched antibody IgG2c and the immunoglobulin gets trafficked into adipose tissues. IgG2c plays pathogenic role in insulin resistance by inducing inflammation from phagocytosis by macrophages. [8] [19] Since Sema4D is related to antibody production and immunoglobulin class switching by shedding of CD23 [1] [3] [39], Sema4D could affect the metabolic phenotype through regulation of B cell signaling in diet-induced obesity.

Obesity is one of the major factors increasing risks of developing metabolic diseases like nonalcoholic fatty liver disease (NAFLD) and type 2 diabetes mellitus (T2DM). T2DM patients are closely associated with insulin resistance and impaired glucose homeostasis. [14] [16] In the obese state, proliferated and hypertrophied adipocytes make adipose tissues pro-inflammatory. Pro-inflammatory adipose tissues change resident anti-inflammatory immune cells into a pro-inflammatory stage and induce the cells to secret pro-inflammatory chemokines. Therefore,

more pro-inflammatory immune cells like neutrophils, macrophages and T cells are recruited to adipose tissues and enhance the yield of pro-inflammatory cytokines like TNF-α and IL-1β. [13] [14] [17] [18] [19] These cytokines activate IKK/NF-κB signaling and augment the expression of target genes related with insulin resistance. [14] [15] [17] IFN-γ produced by CD3+CD4+ Th1 cells also contributes to adipose tissue inflammation and pro-inflammatory macrophages called M1 macrophages promote insulin resistance through blocking insulin actions. [9] [17] [18] [19] Besides these cells, B cells also acts as pro-inflammatory in the obese state. [9] B2 cells are accumulated and activated by leukotriene B4 pathways during diet-induced obesity and worsen insulin resistance and glucose intolerance. [17] [19] Also, obesity increases the production of autoantibodies and pathogenic immunoglobulins (Fig. 2). [18]

Therefore, we posited that Sema4D would affect the metabolic profiles through modulating B cell signaling in diet-induced obesity since one report discovered the relation between obesity and the expression level of soluble Sema4D. [31] In this study, we developed diet-induced obesity in Sema4D KO mice and demonstrated the role of Sema4D in metabolic homeostasis through B cell responses.

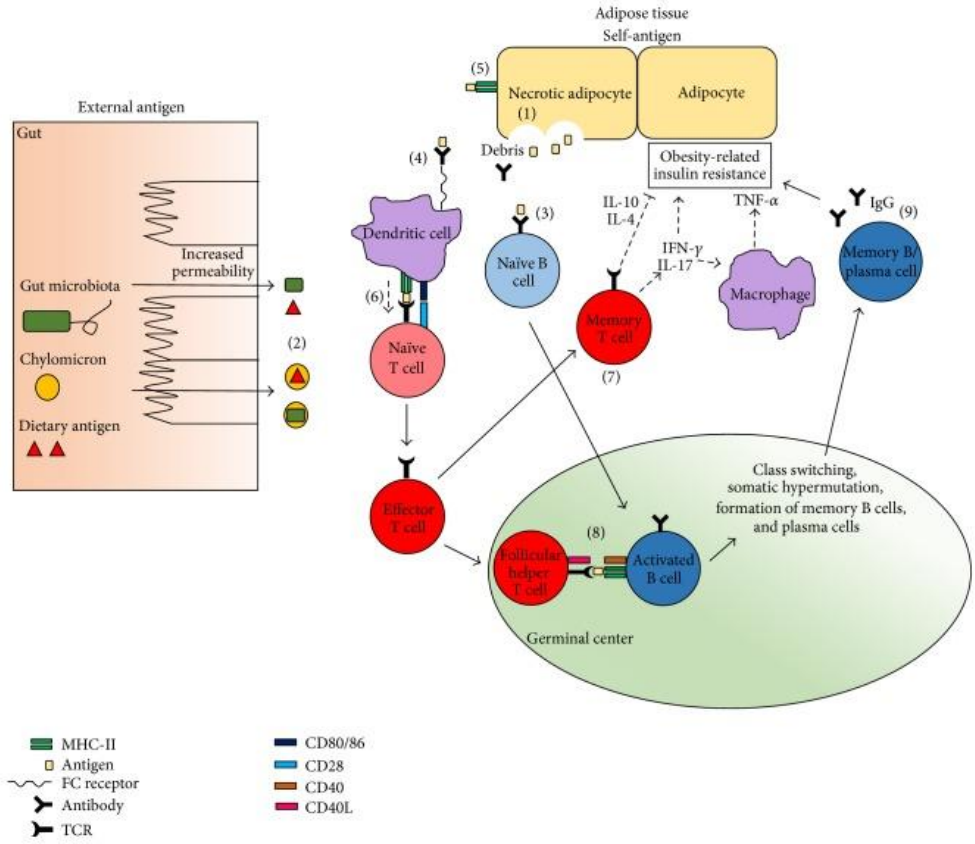

Figure 2. Roles of B cells in developing insulin resistance. (Chng, M. H. et al, Mediators. Inflamm., 2015)

Materials and Methods

Animals

All mice used in this study had a C57BL/6N background. Sema4D KO mice were introduced from MRC Harwell, UK (IMSR 5824) (MOP1607004). Mice were maintained in a specific pathogen free condition and provided food and water ad libitum. 6-week-old male WT and Sema4D KO mice were fed either normal chow diet (NCD; NIH-31, Zeigler, Gardners, PA, USA) or high fat diet (HFD; 20% Protein, 60% Fat, 20% Carbohydrate: D12492, Research Diets, New Brunswick, NJ, USA) for 16 weeks and sacrificed, as described [41, 42]. All these experiments were performed in college of veterinary medicine, Seoul National University, which was accredited by the Ministry of Food and Drug Safety (MFDS, Accredited Unit Number-000011). The experiments were approved by the Institutional Animal Care and Use Committee of Seoul National University (IACUC: SNU-191022-7).

Basal study

Body weight and food intake were measured every week during the diet. Food intake was calculated by subtracting remaining food from the total amounts provided. Fat and spleens were weighted and images were captured after dissected out.

Body composition

Fat masses, lean body masses and free body fluids were assessed by ^{1}H magnetic resonance spectroscopy (Bruker BioSpin, Billerica, MA, USA) after mice were fed 16 weeks of diet.

Metabolic assays

For glucose tolerance tests (GTTs), mice were fasted for 16 hours and injected 0.75mg of glucose (Sigma, Saint Louis, MO, USA) per grams of body weight intraperitoneally. For insulin tolerance tests (ITTs), mice were fasted for 6 hours and injected 1 unit of insulin (Sigma, Saint Louis, MO, USA) per kilograms of body weight intraperitoneally. Glucose levels in blood from tail were measured 0, 15, 30, 60, 90, 120 minutes after glucose or insulin injection with Accu-Check Guide Meter (Roche Diabetes Care, Basel, Switzerland). Area under the curve was calculated with the blood glucose level and the minutes.

Western blotting

For western blotting, total proteins were lysed and extracted using RIPA buffer (Thermo Scientific, Waltham, MA, USA) containing phosphatase inhibitor and protease inhibitor cocktail (GenDEPOT, Barker, TX, USA). Total protein lysates were boiled with 4X Laemmli sample buffer that contained 62.5mM Tris Buffer (pH 6.8), 10% glycerol,

1% lithium dodecyl sulfate (LDS), 0.005% bromophenol blue and distilled water (D.W.). Protein lysates were separated by sodium dodecyl sulfate-polyacrylamide gel electrophoresis and transferred to a polyvinylidene fluoride (PVDF) membrane (Millipore, Billerica, MA, USA). The PVDF membrane blots were blocked in 5% skim milk in Tris-buffered saline with Tween20 (TBS-T) and subjected to immunoblot analysis. Membranes were incubated in 4°C overnight (12~16 hours) with diluted primary antibodies and rinsed 3~4 times with TBS-T. Peroxidase labeled anti-rabbit IgG (PI-1000, Vector Labs, Burlingame, CA, USA), peroxidase labeled anti-mouse IgG (PI-2000, Vector Labs, Burlingame, CA, USA) were used as secondary antibodies. Membranes were incubated with secondary antibodies at room temperature for 1~2 hours and rinsed 3~4 times with TBS-T. Immunoreactive signals were detected and visualized by enhanced chemiluminescence (Abclon, Seoul, Korea) using MicroChemi 4.2 system (DNR Bio-Imaging Systems, Jerusalem, Israel). The specific antibodies used for western blotting are listed in Table 1. The intensity values of protein bands were analyzed with Image J software (National Institutes of Health, Bethesda, MD, USA).

Quantitative real time PCR (qPCR)

Total RNA was extracted and isolated using a total RNA purification system (Invitrogen, Carlsbad, CA, USA) following to the manufacturer's

protocol. Extracted mRNA was reverse-transcribed using AccuPower CycleScript RT PreMix (Bioneer, Daejeon, Korea). Quantitative PCR was performed with ABI StepOne Real-Time PCR instrument (Applied Biosystems, Cheshire, UK) using SYBR Green dye (Bioline, London, UK). For relative quantification of target gene expression, we used the comparative Ct method (Δ ΔCt) and normalized target gene expression to that of the control gene (36B4). Primers were designed according to published complementary DNA or genomic sequences. The specific primer sequences used for PCR are listed in Table 2.

Tissue preparation

Spleen and adipose tissue samples were dissected out and fixed in 4% paraformaldehyde in 0.1M phosphate-buffered saline (PBS, pH 7.4). The fixed samples were embedded in paraffin using embedding center (Leica, Wetzlar, Germany). Paraffin-embedded spleens and adipose tissues were sectioned on a microtome (Leica, Wetzlar, Germany) into 3 and 5 μm coronal section respectively and placed on slide glasses. All sections were processed carefully under the same conditions.

Immunohistochemistry

For accurate immunohistochemistry data, all sections from each group were processed under the same conditions in order to be

comparable. Paraffin sectioned samples were deparaffinized with xylene and rehydrated with graded ethanol from 100 to 50%. The samples were preincubated with quenching buffer (3% H_2O_2 in methyl alcohol) for 20 minutes and blocking buffer (10% normal goat serum in PBS, Vector Labs, Burlingame, CA, USA) for 1 hour at room temperature. Samples were then treated with the primary antibodies against Sema4D (1:200, Biolegend 147604) or F4/80 (1:200, Santacruz sc-59171) overnight at 4°C [43]. Subsequently, the samples were treated with a biotinylated anti-rat IgG and a streptavidin-peroxidase complex (1:200, Vector Labs, Burlingame, CA, USA). Sections were visualized by reaction with 3,3'-diaminobenzidine tetrachloride (Vector Labs, Burlingame, CA, USA), stained with Mayer's Hematoxylin (Thermo Fisher Scientific, Waltham, MA, USA), dehydrated by series of graded ethanol from 50 to 100%, cleaned with xylene and mounted with permount mounting solution (Thermo Fisher Scientific, Waltham, MA, USA). The images were obtained using Pannoramic SCAN (3D Histech, Budapest, Hungary) and captured by CaseViewer software (3D Histech, Budapest, Hungary).

Hematoxylin and eosin staining

Tissue sections were deparaffinized with xylene and rehydrated by gradient of ethanol from 100 to 70%. Samples were stained with filtered Harris hematoxylin (BBC Biochemical, Mount Vernon, WA,

USA) for 3 min, eosin (BBC Biochemical, Mount Vernon, WA, USA) for 1min and washed excess dye with 1% HCl [44] [45]. Thereafter, stained tissues were dehydrated with serial ethanol, cleaned with xylene and mounted with permount mounting solution (Thermo Fisher Scientific, Waltham, MA, USA). The images were obtained using Pannoramic SCAN (3D Histech, Budapest, Hungary) and captured with CaseViewer software (3D Histech, Budapest, Hungary). The lengths were measured by Image J software (National Institutes of Health, Bethesda, MD, USA) and the sizes were analyzed with Image-ProPlus 10.0 software (Media Cybernetics, Silver Spring, MD, USA).

ELISA

IgG2c, IgM, IgA levels were determined in Serum and eWAT lysates using commercially available ELISA kits according to the manufacturer's instructions (Bethyl Laboratories, Montgomery, TX, USA).

Cell preparations and flow cytometry analysis

Spleens were chopped and filtered using 100μm meshes (Cell strainer BD Falcon, Franklin Lakes, NJ, USA). The filtered cells were centrifuged at 1000g for 10 minutes at 4°C. Red blood cells were lysed in 1X RBC lysis buffer (eBioscience 00-4300-54, San Diego, CA, USA) for 5 minutes on ice and filtered through 100μm meshes to generate

single-cell suspensions. Cells were diluted to 1 x 10^6 cells/100ul in Dulbecco's Modified Eagle's Medium (DMEM, 4.5g/L glucose, 4mM glutamine) containing 10% FBS. The cells were stained with the indicated fluorochrome conjugated antibodies after blocking Fc receptors using TruStain FcX (Biolegend 101320). The antibodies used for flow cytometry were PE-conjugated anti-CD138 (Biolegend, 142504), PE/CF594-conjugated anti-CD23 (BD Bioscience, 563986), APC-conjugated anti-CD19 (Biolegend, 115512), PerCP/Cy5.5-conjugated anti-CD5 (eBioscience, 45-0051-82), PE-conjugated anti-IgM (Biolegend, 406508), PE/Dazzle594-conjugated anti-IgD (Biolegend, 405742), PerCP/Cy5.5-conjugated anti-IgG (Biolegend, 405314), and APC/Cy7-conjugated anti-CD45 (Biolegend, 103116). Flow Jo.

Indirect calorimetry study

Oxygen consumption (VO_2), carbon dioxide production (VCO_2), heat production (Energy Expenditure), activity and respiratory exchange ratios (RER) were measured using an indirect calorimetry system (TSE Systems, Bad Homburg, Germany) installed. Mice in each chamber were maintained under 12h light/dark cycle with a constant environmental temperature (22°C) and free access to food and water.

Statistics

All values were expressed as the mean ± SEM. Statistical analysis was performed using Student's T-Test between two groups. The Kruskal-Wallis test was used for flow cytometry analysis. $P < 0.05$ was considered significant.

Table 1. Antibodies used for western blotting

Protein	Gene ID	Company	Catalog No.	Source
CD72	12517	Abcam	ab201079	Rabbit
IFN-gamma	15978	Abbiotec	250708	Rabbit
NF-κB p65	19697	Cell Signaling	#8242	Rabbit
Phospho-NF-κB p65 (Ser536)	19697	Cell Signaling	#3033	Rabbit
Sema4D	20354	Cell Signaling	#82951	Rabbit
Phospho-Shp-1 (Tyr564)	15170	Cell Signaling	#8849	Rabbit
Phospho-Src (Tyr416)	20779	Cell Signaling	#6943	Rabbit
β-Actin	11461	Sigma	A5441	Mouse
GAPDH	14433	Cell Signaling	#2118	Rabbit

Table 2. Primer sequences for quantitative real time PCR

Protein	Forward (5' → 3')	Reverse (5' → 3')
Abhd5	TGGTGTCCCACATCTACATCA	CAGCGTCCATATTCTGTTTCCA
Ccl2	GCTCAGCCAGATGCAGTTA	CTGCTGGTGATCCTCTTGTAG
CD23	AAGATCCAGGTCCGAAAGGC	TCTGAAGCTACTGGGGTGGT
CD72	GGCTGACGCTATCACGTATG	CCTCACAGTCCTGTCCTAGAT
C/ebpα	GACATCAGCGCCTACATCGA	TCGGCTGTGCTGGAAGAG
Dgat2	TCTCAGCCCTCCAAGACATC	GCCAGCCAGGTGAAGTAGAG
Hsl	GGAGCACTACAAACGCAAC	TCCCGTAGGTCATAGGAGAT
Ifn-γ	CACACCTGATTACTACCTTCTTC	GGGTTGTTGACCTCAAACT
IL-1β	GGGCCTCAAAGGAAAGAATC	TCTTCTTTGGGTATTGCTTGG
Plin1	CAGTTCACAGCTGCCAATGAG	ATGGTGCCCTTCAGTTCAGAG
Plin2	GACCTTGTGTCCTCCGCTTAT	CAACCGCAATTTGTGGCTC
Pparγ	TGTGGGGATAAAGCATCAGG	CCGGCAGTTAAGATCACACC
36B4	GAGGAATCAGATGAGGATATGGGA	AAGCAGGCTGACTTGGTTGC

Results

Sema4D expression is increased in the spleen of HFD-fed mice

To investigate the metabolic role of Sema4D, we first verified the expression pattern of Sema4D and its receptor CD72 in various tissues. Sema4D expression appeared in brain, spleen, thymus, and kidney as previous studies addressed (Fig. 3A). Also, CD72 expression was found only in spleen where B cells exist (Fig. 3A). Therefore, interaction between Sema4D and CD72 was sought in spleen (Fig. 3B) since there was no expression of Sema4D and CD72 in epididymal white adipose tissue (eWAT) and none of CD72 in thymus.

Next, we fed 6 weeks old C57BL/6N mice for 16 weeks with normal chow diet (NCD) or 60% high fat diet (HFD) ad libitum to find the change of Sema4D expression in spleen. First, immunoblotting assay was proceeded and found that protein expression level of Sema4D was increased upon HFD challenge (Fig. 3C). Next, spleen sections were stained with Sema4D to conduct immunohistochemical assay. We consistently found that Sema4D expression was greatly increased when HFD was given (Fig. 3D). Finally, to confirm the change of Sema4D expression in splenocytes upon HFD, Sema4D expression in splenocytes was analyzed by flow cytometry analysis. And increase of

Sema4D expression in splenocytes upon HFD was ascertained (Fig. 3E).

A

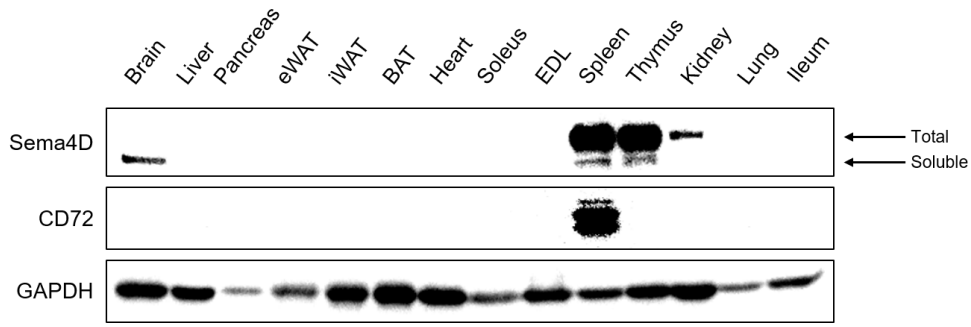
Brain
Liver
Pancreas
eWAT
iWAT
BAT
Heart
Soleus
EDL
Spleen
Thymus
Kidney
Lung
Ileum
Sema4D
CD72
GAPDH
Total
Soluble

B

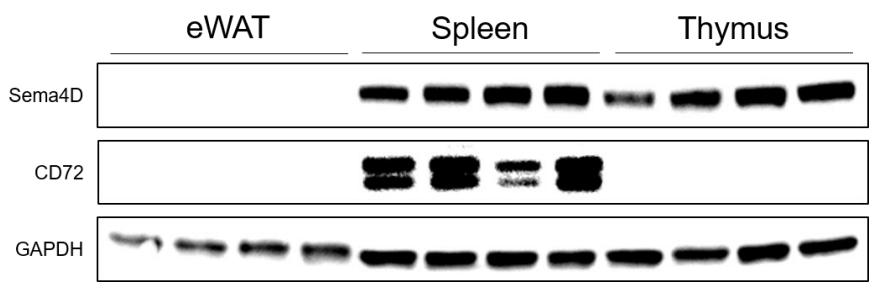
eWAT
Spleen
Thymus
Sema4D
CD72
GAPDH

C

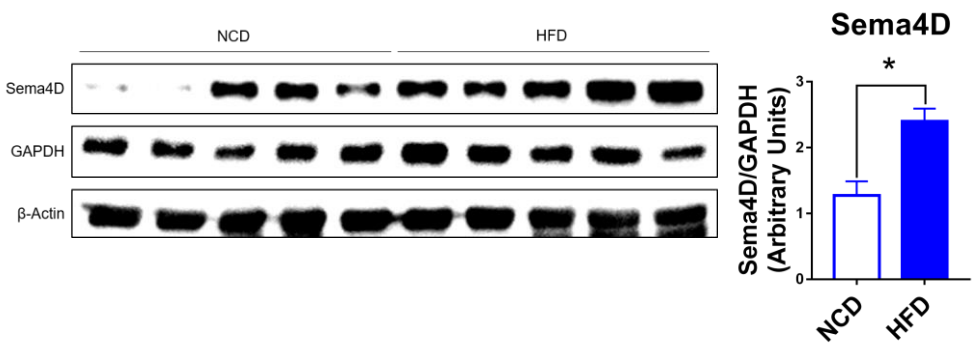
NCD
HFD
Sema4D
GAPDH
β-Actin
Sema4D
*
Sema4D/GAPDH (Arbitrary Units)
3
2
1
0
NCD
HFD

D

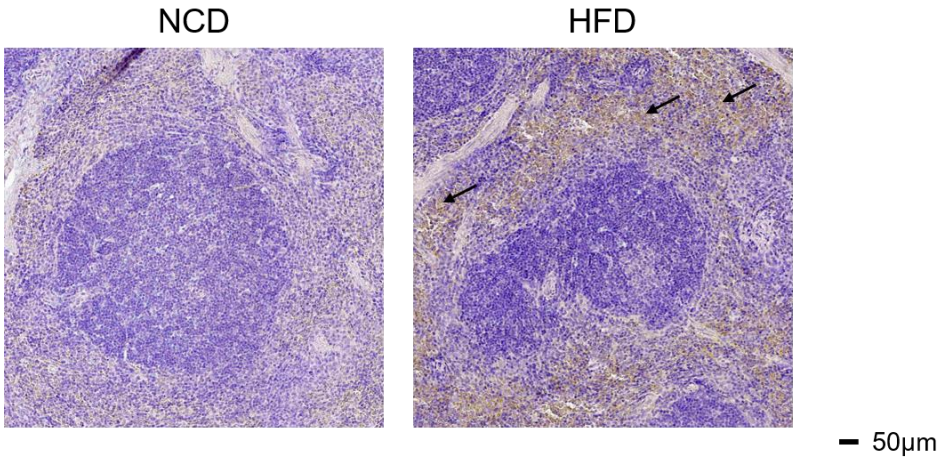
NCD
HFD
50μm

E

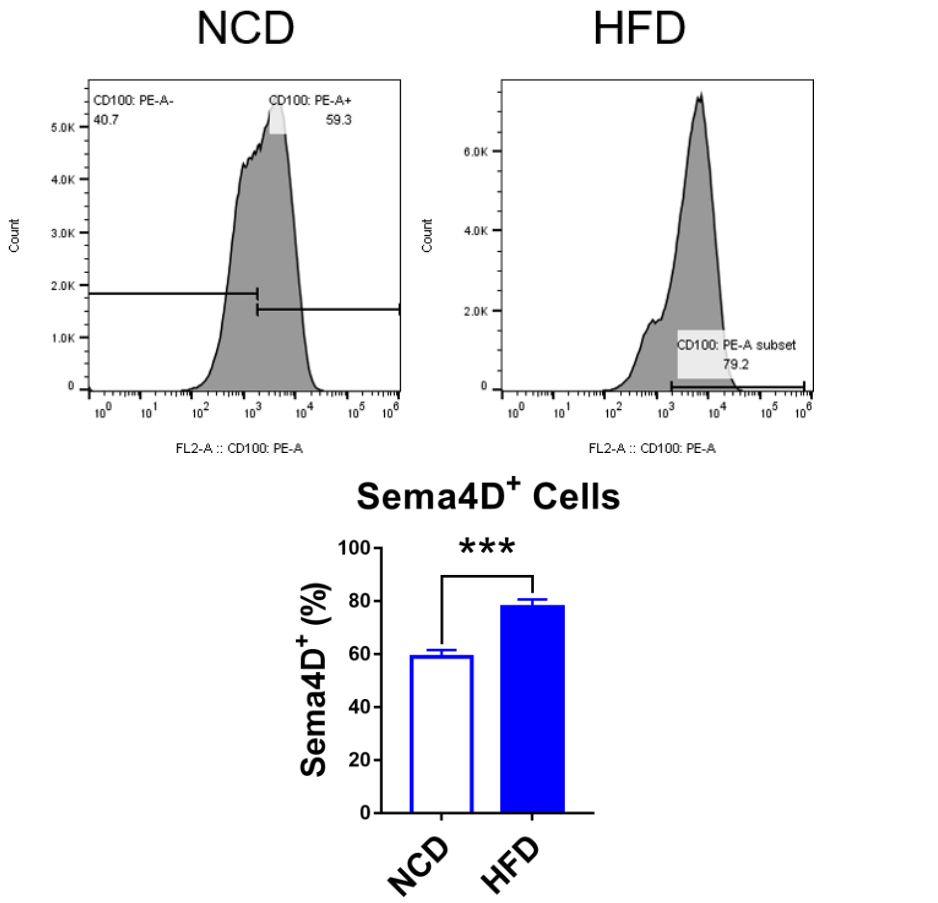
NCD
HFD
CD100: PE-A-
40.7
CD100: PE-A+
59.3
Count
FL2-A :: CD100: PE-A
CD100: PE-A subset
79.2
Sema4D+ Cells
***
Sema4D+ (%)
NCD
HFD

Figure 3. Sema4D expression is increased in the spleen of HFD WT compared to NCD WT.

(**A**) Protein expression pattern of Sema4D and CD72 in various tissues from 8-week-old C57BL/6N. (**B**) Protein expression of Sema4D and CD72 in epididymal adipose tissue, spleen, and thymus from 8 weeks old C57BL/6N mice. (**C**) Protein expression of Sema4D (left) and relative expression level of Sema4D to GAPDH (right). (**D**) Immunohistochemical analysis of Sema4D in WT NCD and HFD spleen (arrow). (**E**) Flow cytometry analysis of Sema4D in WT NCD and HFD splenocytes. Representative images from FlowJo (above). Data are the means ± standard error of means (SEM); *P < 0.05, **P < 0.01, ***P < 0.001. significant.

Sema4D KO mice gained less body weight and showed improved glucose intolerance

Next, Sema4D critical gene deletion mice (Sema4D KO) were obtained and 6-week-old C57BL/6N or Sema4D KO mice were fed with normal chow diet or 60% high fat diet for 16 weeks. When given HFD, Sema4D KO mice gained less body weight compared to wild type mice whereas food intake did not show significant differences between WT and KO (Fig. 4A, B). For further analyzation, the body composition of WT and Sema4D KO fed NCD or HFD were conducted. Significant decrease in the fat mass and fat-to-body ratio in HFD Sema4D KO was observed compared to HFD WT (Fig. 4C). This decrease was invariably shown with the epididymal fat pads (Fig. 4D). Consistent with the decrease of the fat mass, the frequencies of smaller adipocytes in KO mice were higher in both NCD and HFD adipocytes and this was confirmed by the respiratory exchange ratio (Fig. 4E, F). Furthermore, when expression of genes related to adipogenesis and lipid metabolism were analyzed, HFD Sema4D KO expressed less compared to HFD WT (Fig. 4G). To find out whether the decrease of adipose tissue affected glucose homeostasis, glucose tolerance test and insulin tolerance test were conducted. Fasting blood glucose level of HFD Sema4D KO mice was lower than HFD WT mice (Fig. 4H). Also, HFD Sema4D KO mice recovered blood glucose level much faster than HFD WT mice upon glucose injection (Fig. 4I) and insulin

injection (Fig. 4J). Therefore, HFD Sema4D KO mice were protected from glucose intolerance and insulin resistance and metabolic phenotype like body weight and fat mass were ameliorated by improved lipid metabolism.

A

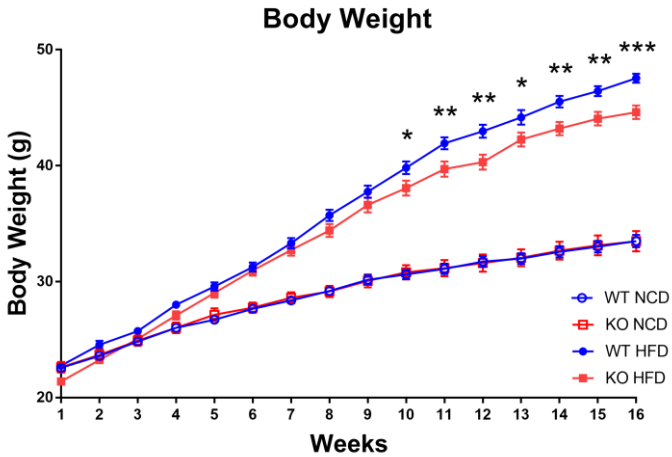
Body Weight
Body Weight (g)
Weeks
WT NCD
KO NCD
WT HFD
KO HFD
*
**
**
*
**
**
***

B

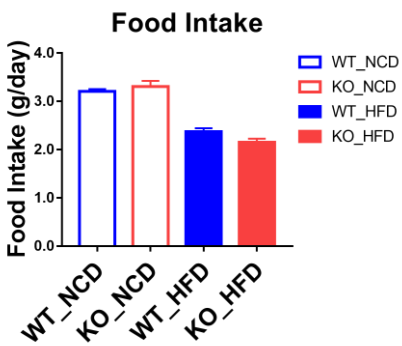
Food Intake
Food Intake (g/day)
WT_NCD
KO_NCD
WT_HFD
KO_HFD

C

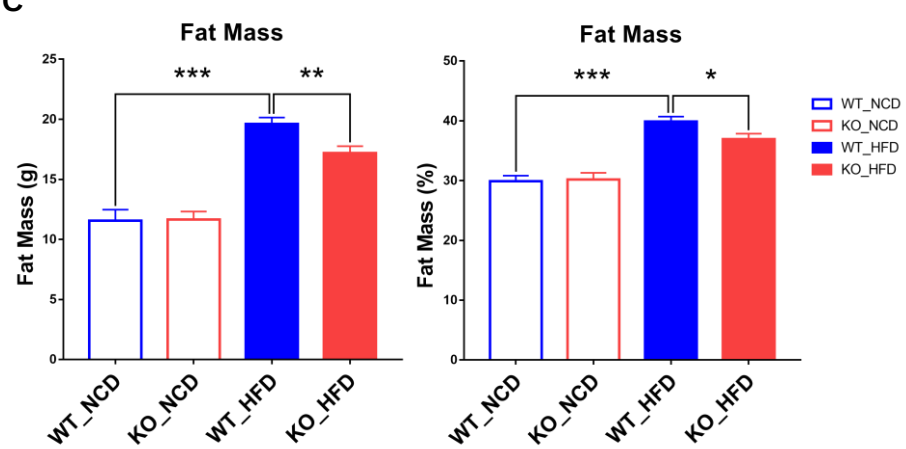
Fat Mass
Fat Mass (g)
***
**
Fat Mass
Fat Mass (%)
***
*
WT_NCD
KO_NCD
WT_HFD
KO_HFD

D

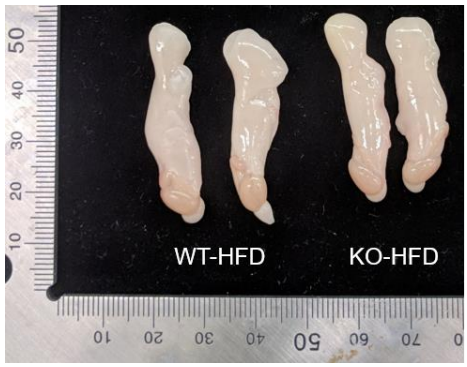

Epididymal
WAT

E

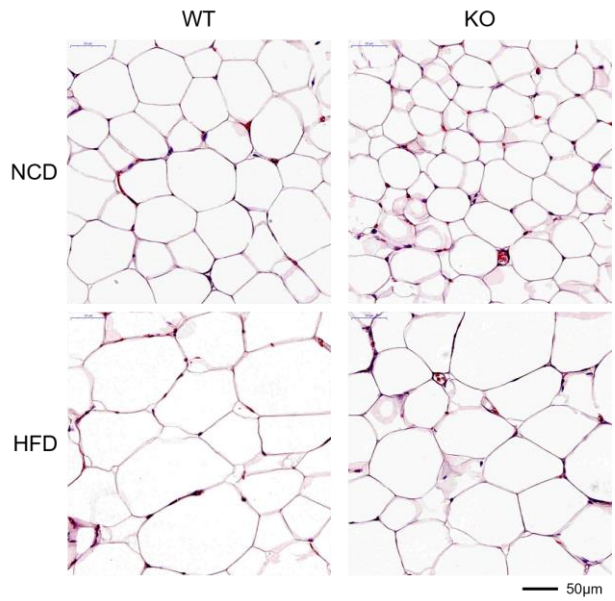

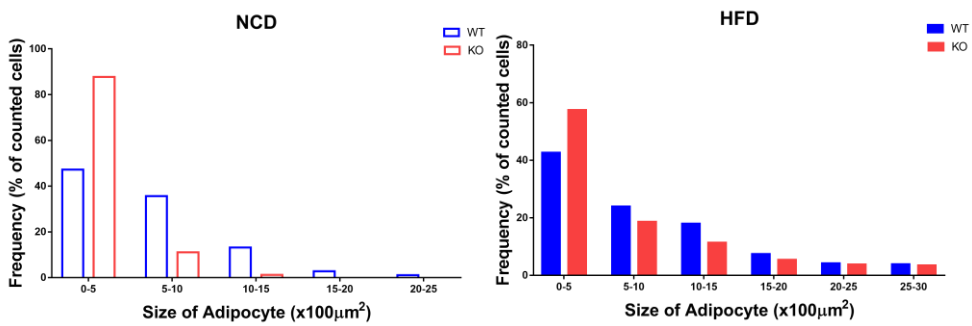

F

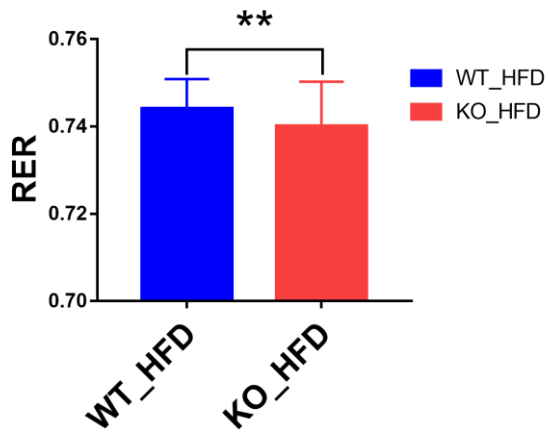
**
0.76
0.74
0.72
0.70
RER
WT_HFD
KO_HFD
WT_HFD
KO_HFD

G

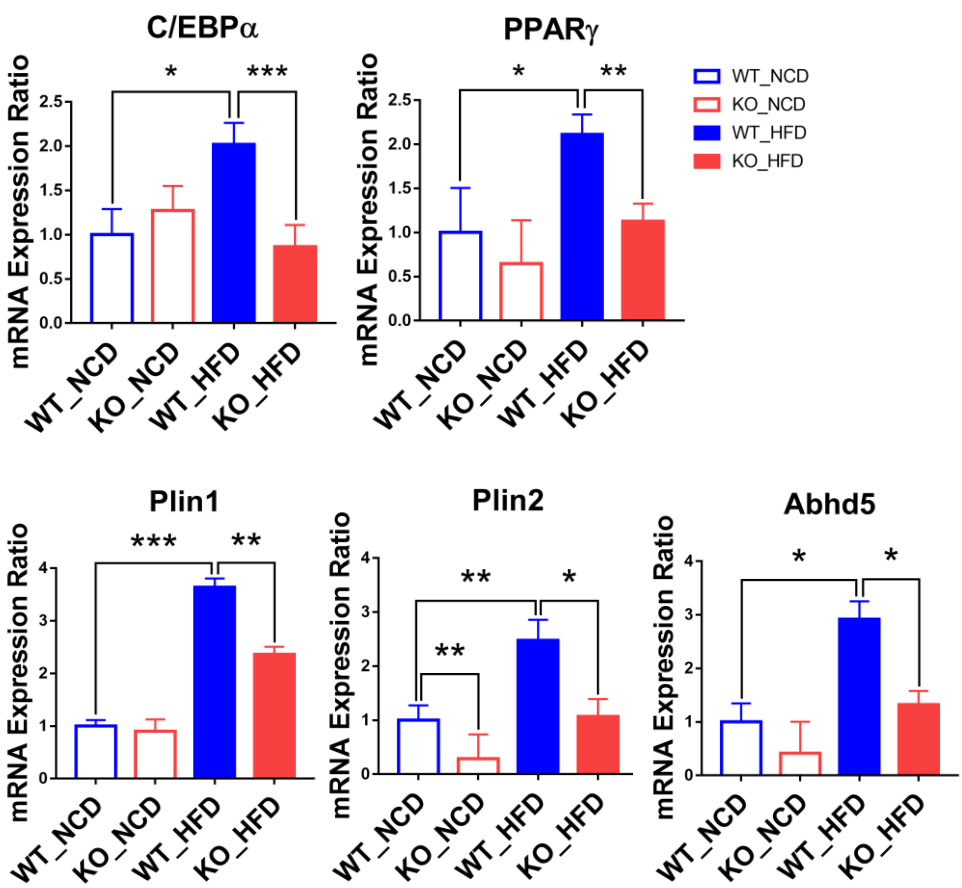
C/EBPα
PPARγ
mRNA Expression Ratio
WT_NCD
KO_NCD
WT_HFD
KO_HFD
Plin1
Plin2
Abhd5

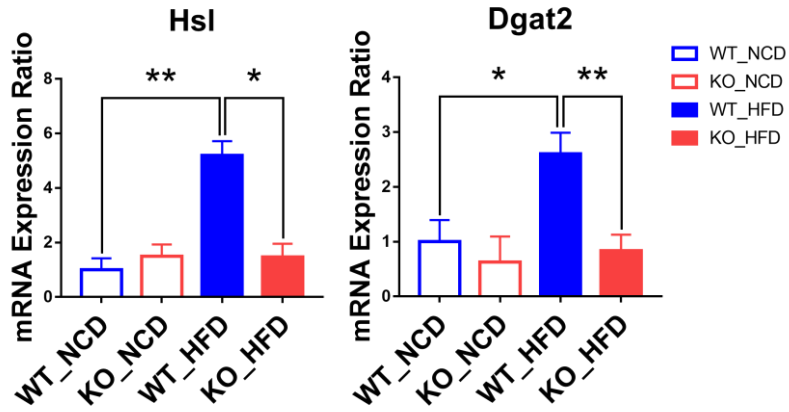
Hsl
Dgat2
mRNA Expression Ratio
mRNA Expression Ratio
**
*
*
**
WT_NCD
KO_NCD
WT_HFD
KO_HFD
WT_NCD
KO_NCD
WT_HFD
KO_HFD
WT_NCD
KO_NCD
WT_HFD
KO_HFD

H

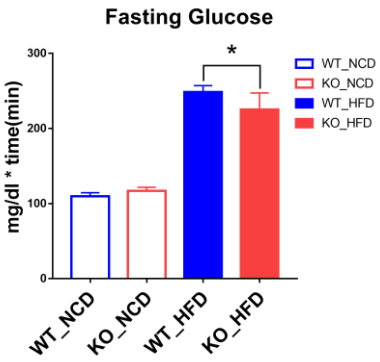
Fasting Glucose
mg/dl * time(min)
*
WT_NCD
KO_NCD
WT_HFD
KO_HFD
WT_NCD
KO_NCD
WT_HFD
KO_HFD

I

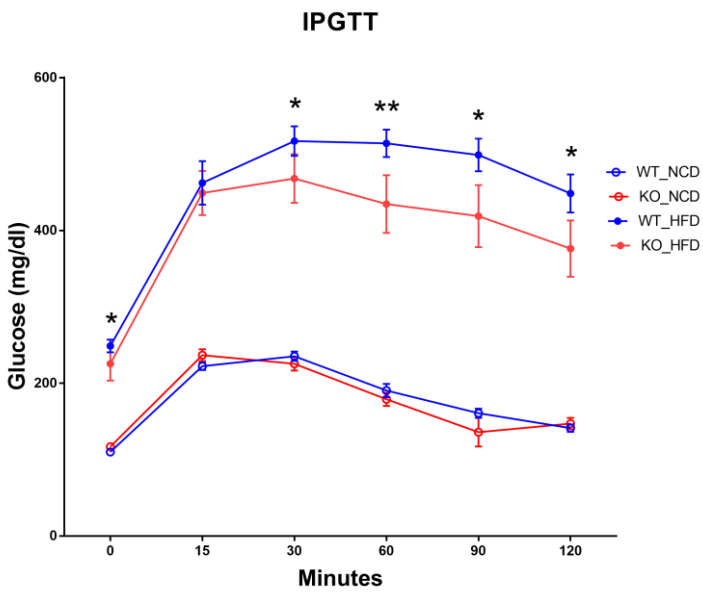
IPGTT
Glucose (mg/dl)
Minutes
*
*
**
*
*
WT_NCD
KO_NCD
WT_HFD
KO_HFD

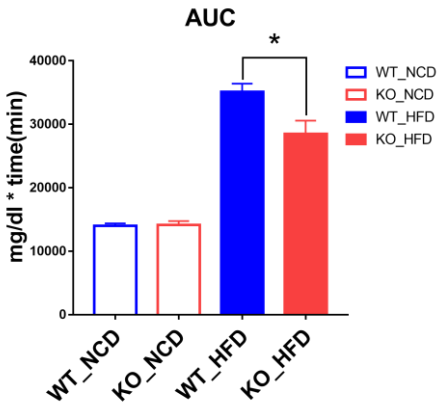
AUC
*
mg/dl * time(min)
40000
30000
20000
10000
0
WT_NCD
KO_NCD
WT_HFD
KO_HFD
WT_NCD
KO_NCD
WT_HFD
KO_HFD

J

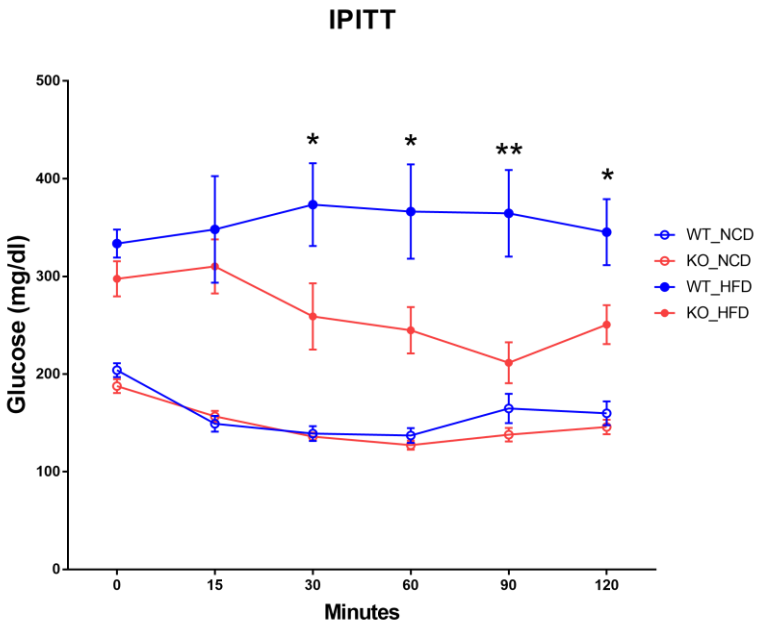
IPITT
Glucose (mg/dl)
500
400
300
200
100
0
*
*
**
*
0
15
30
60
90
120
Minutes
WT_NCD
KO_NCD
WT_HFD
KO_HFD

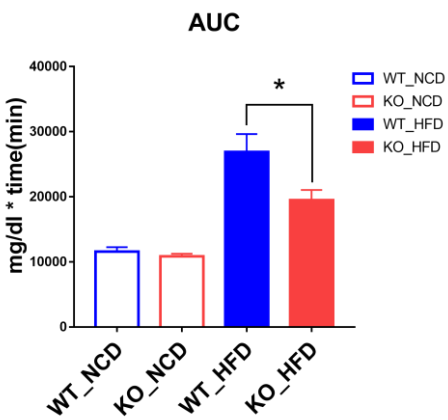
AUC
*
mg/dl * time(min)
40000
30000
20000
10000
0
WT_NCD
KO_NCD
WT_HFD
KO_HFD
WT_NCD
KO_NCD
WT_HFD
KO_HFD

Figure 4. Physiological changes in Sema4D KO mice.

(**A**) Changes in body weights during 16 weeks of NCD or HFD fed male WT or KO mice. (n = 5-8 per group) (**B**) Food intake. (**C**) Body-composition changes in WT and Sema4D KO mice after feeding 16 weeks of diet. (**D**) Representative picture of epididymal white fat pads from mice fed HFD. (**E**) Representative images of H&E staining in epididymal WAT in NCD and HFD Sema4D KO (above) and distribution of adipocyte sizes (below). (**F**) The respiratory exchange ratio in HFD WT and Sema4D KO was calculated as CO2 production/O2 consumption. (**G**) Relative mRNA levels of genes related to lipid metabolism and adipogenesis in eWAT were measured by qPCR. The values were normalized to 36B4. (**H**) Fasting blood glucose levels. (**I**) Glucose tolerance test of WT or KO mice after 16-week NCD or HFD challenge (above) and AUC (below). (**J**) Insulin tolerance test of WT or KO mice after 16-week HFD challenge (above) and AUC (below). Graphs are presented as means ± SEM; *P < 0.05, **P < 0.01, ***P < 0.001.

Inflammation is reduced in the spleen of HFD-fed Sema4D KO mice

Sema4D plays crucial role in B cell responses. Therefore, spleens from WT or Sema4D KO mice given NCD or HFD were isolated to determine the level of inflammation.

The mRNA expression level of pro-inflammatory cytokines such as IL-1β and IFN-γ were decreased in the spleen from HFD Sema4D KO (Fig. 5A) and the activation of NF-κB p65 subunit was consistent with the mRNA data (Fig. 5B). Since it is known that Sema4D interacts with its receptor CD72 especially expressing on B cells [3] [12] [20] [23], we hypothesized that the decrease of systemic inflammation in HFD Sema4D KO came from the reduction of immune responses in spleen. Therefore, hematoxylin and eosin staining was proceeded with spleen sections and the average area of white pulp was decreased in HFD Sema4D KO, which means that the interaction between T cells and B cells in spleen was decreased. In summary, deletion of Sema4D reduced systemic inflammation through decreased immune response in diet-induced obesity.

A

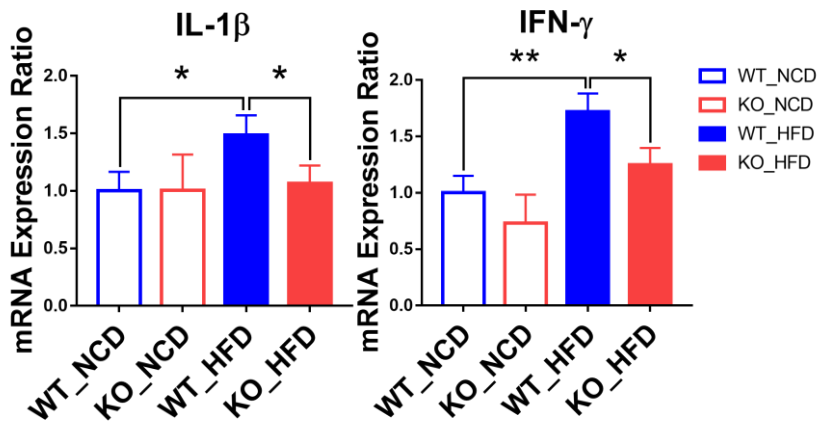
IL-1β
IFN-γ
mRNA Expression Ratio
2.0
1.5
1.0
0.5
0.0
*
*
**
*
WT_NCD
KO_NCD
WT_HFD
KO_HFD

B

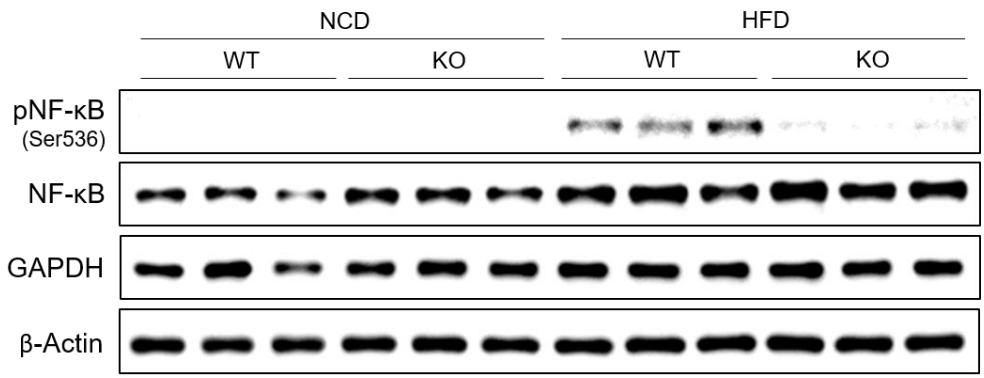
NCD
HFD
WT
KO
WT
KO
pNF-κB
(Ser536)
NF-κB
GAPDH
β-Actin

C

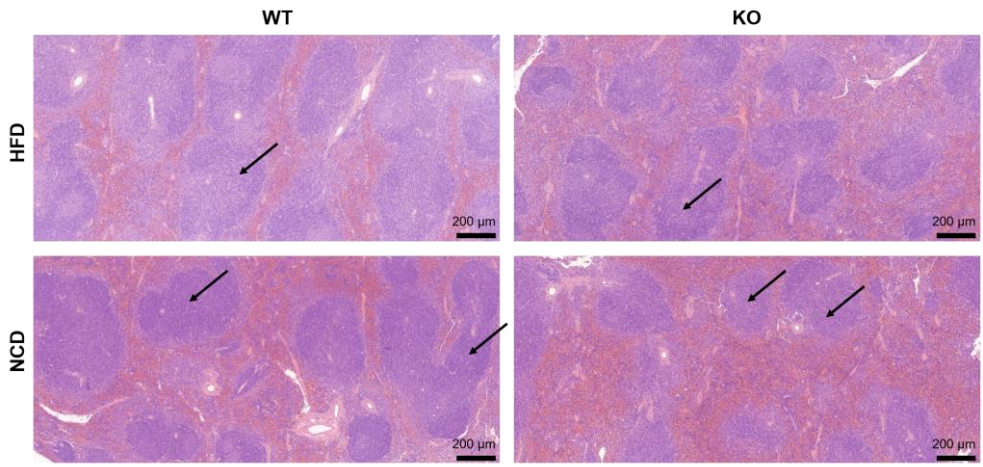
WT
KO
HFD
NCD
200 μm

Figure 5. Inflammation is decreased in the spleen of HFD-fed Sema4D KO mice.

(**A**) qPCR analysis of IL-1β and IFN-γ in spleen of WT or KO mice on 16-week NCD or HFD; expression was normalized to that of 36B4. (**B**) Phosphorylated NF-κB p65 subunit level was assessed by immunoblotting in spleen. (**C**) Representative H&E staining images of NCD and HFD Sema4D WT and KO spleens (arrow: white pulp). Data are shown as means ± SEM; *P < 0.05, **P < 0.01, ***P < 0.001.

Decreased inflammation is derived from immature B cell development in HFD-fed Sema4D KO spleen

We have shown that the interaction between immune cells was decreased in spleen (Fig. 5C). Therefore, we wondered whether decreased interaction had affected spleen morphology and the size of spleens was increased in HFD Sema4D KO (Fig. 6A). Spleen weights of both NCD and HFD Sema4D KO were heavier than those of NCD or HFD WT (Fig. 6B). For further investigation, B cell population in the spleen was analyzed to verify the reason spleens were bigger in Sema4D KO. The mRNA level of CD19 was higher in HFD Sema4D KO and the percentages of B cells in splenocytes were also higher in Sema4D KO (Fig. 6C). Since B cell population was increased, B cell signaling might have been affected by change of the population. Gene expression and protein expression of CD72 were found to be increased in HFD Sema4D KO (Fig. 6D). Next, to ascertain whether B cell signaling had been modulated, levels of phosphorylated Shp-1 and Src were analyzed with immunoblotting assay. Phosphorylation of Shp-1 and Src were increased in HFD Sema4D KO which means that the deletion of Sema4D reduced B cell responses (Fig. 6E).

Sema4D is known to promote immunoglobulin class switching to IgG and IgE by inducing shedding of CD23 on B cell plasma membranes [1] [3] [20] [28] [32] [33] [36] [37] [38]. Therefore, we sought to find whether Sema4D affected B cell proliferation and further differentiation into plasma cells

and isotype class switching via shedding of CD23. The mRNA level of CD23 in spleens was examined and CD23 mRNA level in HFD Sema4D KO was lower than that in HFD WT (Fig. 6F). Nevertheless, the percentages of CD23+ cells in splenocytes were higher in Sema4D KO (Fig. 6F), indicating that Sema4D KO produces more B cells but has less capability of differentiating B cells into class switched plasma cells through reduced B cell responses. Since Sema4D KO differentiated smaller number of B cells and less class switched, the serum levels of antibodies were examined. Class switched antibody IgG2c which is known to have pathogenic roles [8] [27] was produced less in Sema4D KO mice even though natural antibodies IgM and one of class switched antibody IgA level were unaffected (Fig. 6F). Collectively, Sema4D KO mice had more B cells but signaling in the B cells were decreased. Decreased responses caused the B cells not to differentiate into plasma cells nor to produce class switched immunoglobulins.

A

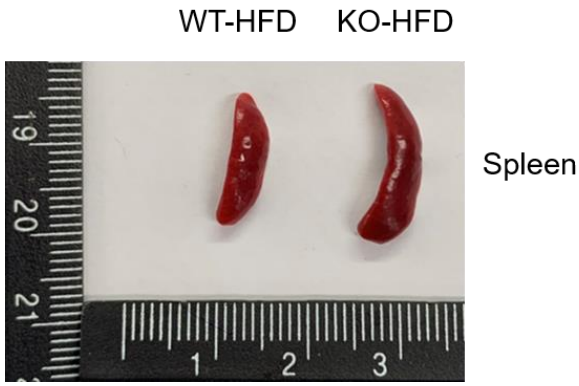
WT-HFD
KO-HFD
Spleen

B

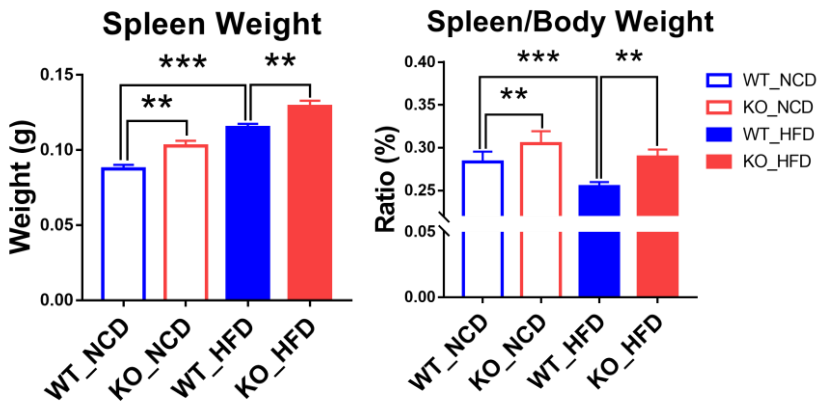
Spleen Weight
Weight (g)
0.15
0.10
0.05
0.00
***
**
**
WT_NCD
KO_NCD
WT_HFD
KO_HFD
Spleen/Body Weight
Ratio (%)
0.40
0.35
0.30
0.25
0.05
0.00
***
**
**
WT_NCD
KO_NCD
WT_HFD
KO_HFD

C

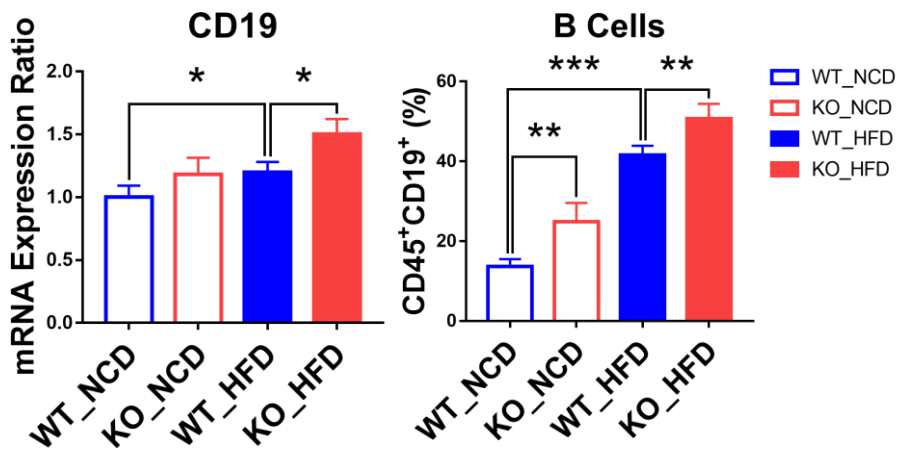
CD19
mRNA Expression Ratio
2.0
1.5
1.0
0.5
0.0
*
*
WT_NCD
KO_NCD
WT_HFD
KO_HFD
B Cells
CD45+CD19+ (%)
60
40
20
0
***
**
**
WT_NCD
KO_NCD
WT_HFD
KO_HFD

D

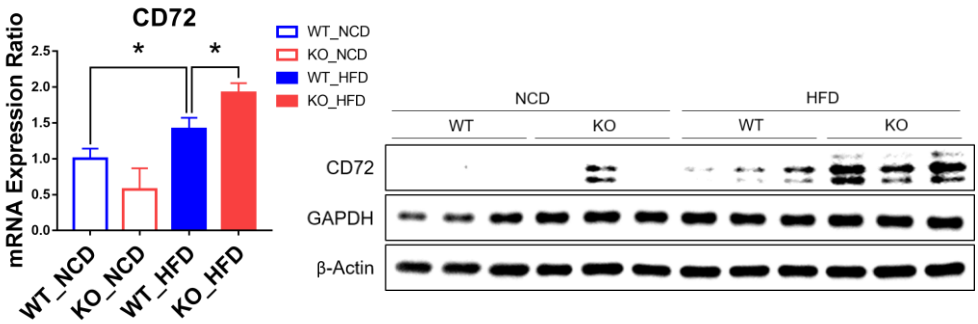
CD72
mRNA Expression Ratio
2.5
2.0
1.5
1.0
0.5
0.0
*
*
WT_NCD
KO_NCD
WT_HFD
KO_HFD
WT_NCD
KO_NCD
WT_HFD
KO_HFD
NCD
HFD
WT
KO
WT
KO
CD72
GAPDH
β-Actin

E

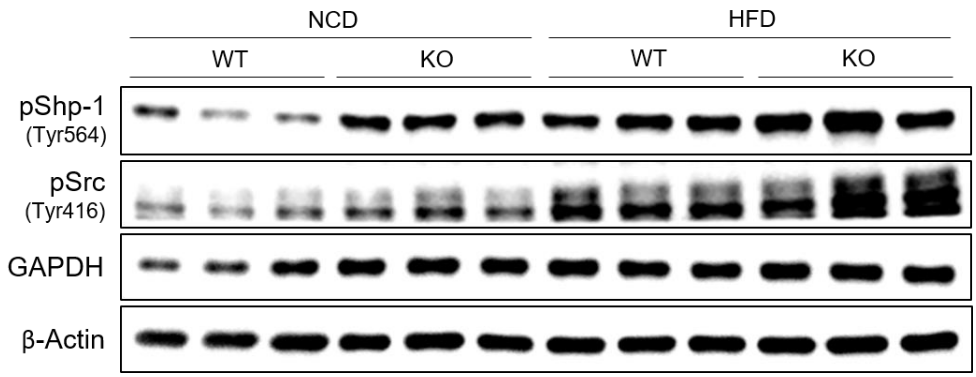
NCD
HFD
WT
KO
WT
KO
pShp-1
(Tyr564)
pSrc
(Tyr416)
GAPDH
β-Actin

F

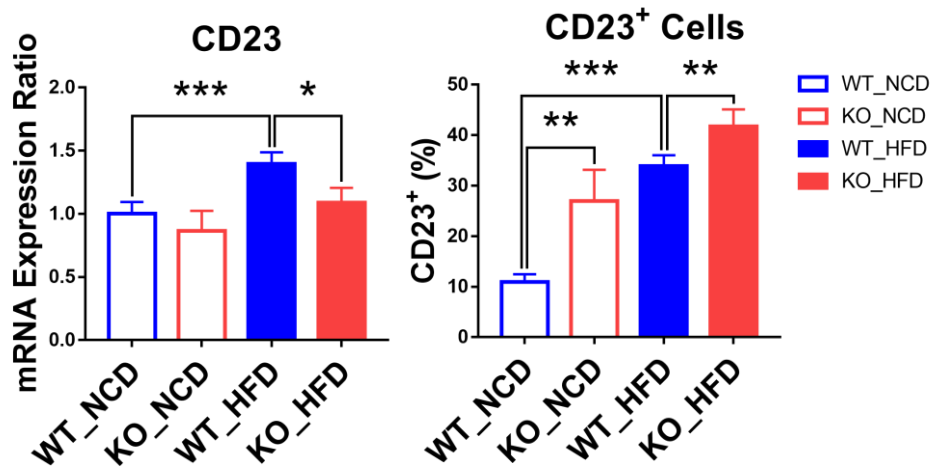
CD23
mRNA Expression Ratio
2.0
1.5
1.0
0.5
0.0
***
*
WT_NCD
KO_NCD
WT_HFD
KO_HFD
CD23+ Cells
CD23+ (%)
50
40
30
20
10
0
***
**
**
WT_NCD
KO_NCD
WT_HFD
KO_HFD

G

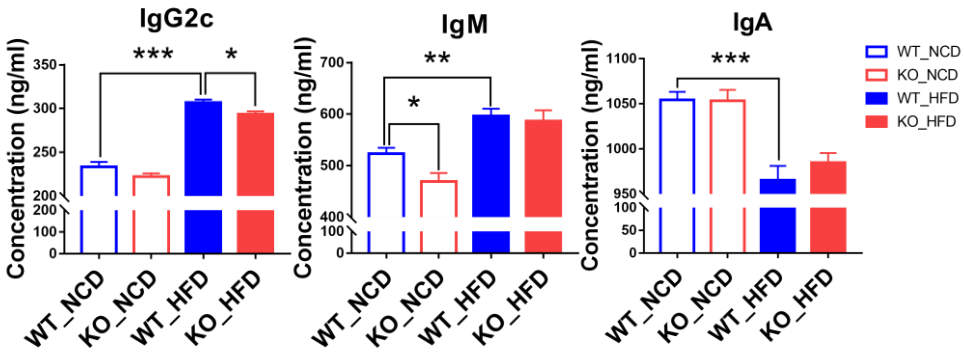

Figure 6. B cell differentiation is changed in Sema4D KO mice.

(**A**) Representative image of spleens from HFD WT and HFD Sema4D KO. (**B**) Spleen weights and spleen index calculated with spleen and body weight. (**C**) qPCR analysis of CD19 in spleen of WT or KO mice on 16-week NCD or HFD; expression was normalized to that of 36B4 (left) and flow cytometry analysis of B cell population (CD45+CD19+) in WT or KO mice on NCD or HFD (right). (**D**) mRNA expression (left) and protein expression (right) of CD72 in spleen. (**E**) Phosphorylated Shp-1 (Tyr564) and Src (Tyr416) were analyzed by immunoblotting in spleen. (**F**) qPCR analysis of CD23 in spleen; expression was normalized to that of 36B4 (left) and flow cytometry analysis of CD23+ splenocytes (right). (**G**) IgG2c, IgM, IgA concentrations in mice serum. Data are the means ± SEM; *P < 0.05, **P < 0.01, ***P < 0.001.

Adipose tissue inflammation is alleviated in HFD Sema4D KO through reduction of pathogenic antibodies

We have shown that HFD Sema4D KO had decreased systemic inflammation by inhibited B cell differentiation and class switching in spleen. Thereafter, we wondered whether reduction of systemic inflammation and production of class switched antibody in HFD Sema4D KO would peripherally affect adipose tissue inflammation and drive alleviated glucose intolerance. Hence, level of adipose tissue inflammation was investigated and the mRNA expressions of pro-inflammatory genes were decreased in HFD Sema4D KO epididymal white adipose tissue (Fig. 7A). Consistently, the protein level of IFN-γ was also reduced in HFD Sema4D KO eWAT (Fig. 7B). To confirm the level of inflammation in eWAT, the qPCR analysis of CCL2 and immunohistochemistry analysis of F4/80 were examined. The mRNA level of CCL2 was significantly decreased in Sema4D KO and the numbers of crown like structures (CLS) were highly decreased in HFD Sema4D KO (Fig. 7C).

Next, we evaluated the antibody concentration in eWAT because recent studies have shown that B cells and pathogenic antibodies from diet-induced obesity could accelerate adipose tissue inflammation and glucose intolerance [8] [9] [10] [17] [19] [25] [27]. And concentration of IgG2c, supposed to be pathogenic [8] [27], was diminished in Sema4D KO eWAT even though the natural antibody IgM level was insignificantly

changed between WT and Sema4D KO (Fig. 7D). This result suggested that decreased adipose tissue inflammation was partially resulted from reduced pathogenic IgG2c in adipose tissues and decline of infiltrated macrophages.

A

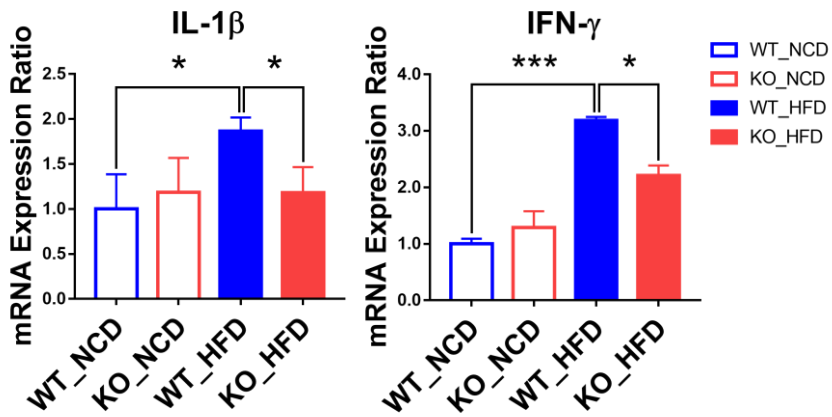
IL-1β
IFN-γ
mRNA Expression Ratio
WT_NCD
KO_NCD
WT_HFD
KO_HFD

B

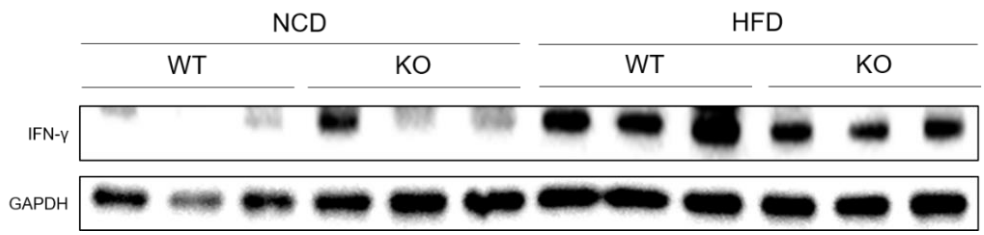
NCD
HFD
WT
KO
IFN-γ
GAPDH

C

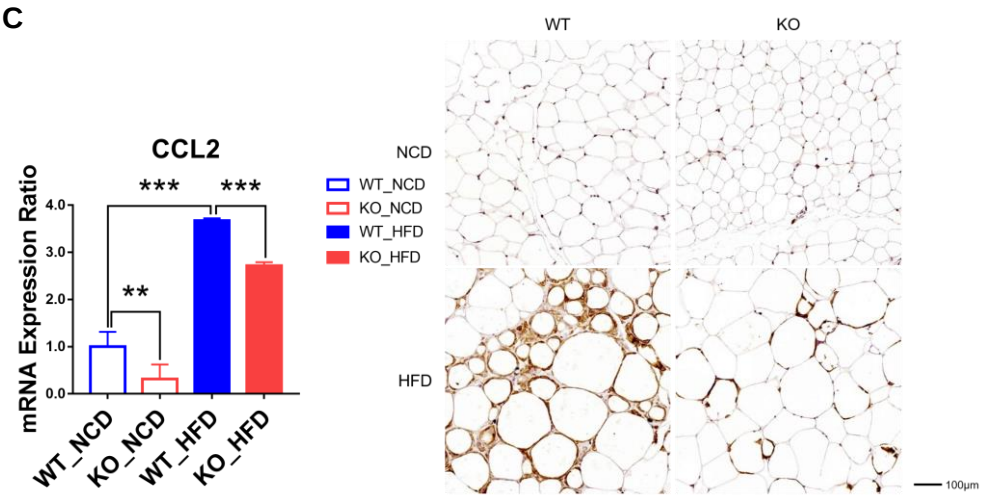
CCL2
mRNA Expression Ratio
WT_NCD
KO_NCD
WT_HFD
KO_HFD
WT
KO
NCD
HFD
100μm

D

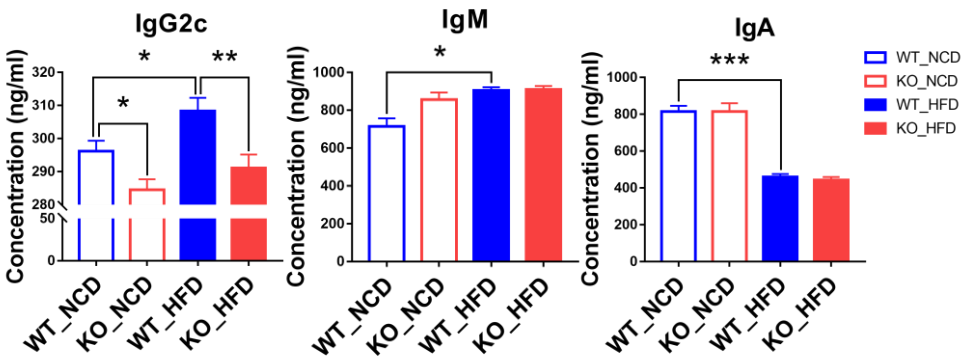

Figure 7. Adipose tissue inflammation is declined in HFD-fed Sema4D KO mice.

(**A**) qPCR analysis of IL-1β and IFN-γ in eWAT of WT or KO mice challenged 16-week NCD or HFD; expression was normalized to that of 36B4. (**B**) Protein level of IFN-γ was analyzed by immunoblotting in eWAT. (**C**) The mRNA expression of CCL2 (left) and immunohistochemical analysis of crown-like structures surrounding adipocytes in Sema4D WT and KO given NCD and HFD; paraffin sectioned eWAT samples were stained with F4/80 (right). (**D**) Concentrations of antibody subtypes in mice eWAT lysates. Data are the means ± SEM; *P < 0.05, **P < 0.01, ***P < 0.001.

Discussion

The metabolic functions of Sema4D have not been understood, nevertheless soluble Sema4D is increased in obese African. [31] In this study, we discovered that Sema4D regulates metabolic phenotype by managing B cell development and inflammation. Sema4D deficiency in diet-induced obesity improved glucose intolerance, insulin resistance and metabolism of adipose tissues. Ablation of Sema4D decreased systemic and adipose tissue inflammation through reduction of B cell development and production of pathogenic antibodies.

Loss of Sema4D decreased systemic inflammation and B cell development in diet-induced obesity. Reduction of B cell differentiation resulted in less production of pathogenic class-switched immunoglobulins. Therefore, smaller number of pathogenic antibodies in adipose tissues induced less adipose tissue inflammation and immune cell infiltration (Fig. 7). Lower level of adipose tissue inflammation inhibited proliferation and hypertrophy of adipocytes and improved lipid metabolism in adipose tissues which were confirmed by the mRNA, histology, and respiratory exchange ratio from indirect calorimetry study. Consumption of more fatty acid affected the size of

adipocytes, mass of adipose tissues and body weight (Fig. 4). Therefore, Sema4D deficiency improved glucose intolerance in diet-induced obesity.

Immune cells have been recognized as critical factors that facilitate adipose tissue inflammation. In obese adipose tissues, infiltrated macrophages and T cells as well as resident immune cells produce pro-inflammatory cytokines that augment adipose tissue inflammation and eventually impair glucose homeostasis. [9] [13] [14] [15] [17] [18] [19] Additionally, B cells also have a part in accelerating adipose tissue inflammation. Previous studies demonstrated that B cells promote insulin resistance by producing and secreting pathogenic immunoglobulins. Class switched antibody IgG2c, which is one of the IgG subclasses, was found to be the major pathogenic immunoglobulin. The IgG2c is phagocytized by macrophages and the macrophages produce pro-inflammatory cytokines that facilitate glucose intolerance and insulin resistance. [8] [9] [17] [19] [25] Here, we also showed that HFD Sema4D KO mice produced lower level of IgG2c (Fig. 6G). Spleen from HFD Sema4D KO mice expressed less CD23 and the proteolysis of CD23 from the splenocytes surface was reduced as well. CD23 expression affects to normal B cell development and B cell receptor could undergo immunoglobulin class switch after CD23 is shed from the surface. Sema4D induces proteolysis of CD23 and thus produces

different isotype immunoglobulins. [1] [3] [12] [20] [23] [39] However, deletion of Sema4D in diet-induced obesity mice inhibited the shedding of CD23 and the production of class switched immunoglobulins (Fig. 6F, G). Furthermore, some reports have showed that spleens from mice that lack activation-induced cytidine deaminase tend to be bigger than those from WT. Differences in spleen masses are thought to be the results of proliferation of inactivated immature B cells. [46] [47] Both Sema4D KO mice fed NCD and HFD had bigger spleens than those from WT mice (Fig. 6A, B). Consistently, the percentages of $CD45^{+}CD19^{+}$ B cells were higher in Sema4D KO than WT (Fig. 6C). Therefore, we could posit that Sema4D KO mice tend to have bigger spleens composed with more immature B cells that could not develop nor differentiate into plasma cells. Nevertheless, it is still essential to verify the numbers of specific B cell subsets following with the lineage to confirm our hypothesis.

In diet-induced obesity, adipocytes proliferate and hypertrophy. Increased adipose tissues become bigger and get pro-inflammatory. Inflammation in adipose tissue is a major factor for developing glucose intolerance and insulin resistance. Immune cells and cytokines promote insulin resistance by blocking insulin action or increasing the expression of genes related to insulin resistance. [9] [13] [14] [15] [17] [18] [19] Adipose tissues from HFD Sema4D KO mice were much less

inflammatory than WT (Fig. 7A~C). Consistently, the sizes of adipocytes (Fig. 4E) and masses of epididymal white adipose tissues (eWAT) were smaller (Fig. 4C, D) and expressions of genes related to lipid metabolism and adipogenesis were also decreased (Fig. 4G). The respiratory exchange ratio confirmed the improved fat metabolism (Fig. 4F). We discovered that the concentration of the pathogenic immunoglobulin IgG2c in eWAT was decreased in HFD Sema4D KO mice (Fig. 7D). We discovered that the decline of adipose tissues inflammation in HFD Sema4D KO was derived from reduced pathogenic IgG2c and infiltrated immune cells (Fig. 7C). And this reduction of inflammation in adipose tissue is thought to be the major regulator of the improved glucose intolerance and insulin resistance in HFD Sema4D KO mice (Fig. 4H ~ J).

Semaphorin family is phylogenetically conserved among many species and thus Sema4D is well conserved in vertebrates too. [1] [3] [20] Therefore, Sema4D has been investigated in several models including human. CD72, the lymphoid receptor of Sema4D, has been studied in human as well. [26] [28] The interaction between Sema4D and CD72 and the impact of the interaction have been researched in autoimmune disease patients. It is known that Sema4D stimulation by immune activation inactivates CD72 and decreased expression of CD72 increases IgG class switching on B cells from lupus nephritis patients.

[28] However, it has not been studied the impact of the interaction between Sema4D and CD72 on obese human. The mRNA level of CD72 in spleen from HFD Sema4D KO mice was increased compared to HFD WT (Fig. 6D). Therefore, more investigation about IgG class switching derived from interaction between Sema4D and CD72 and glucose homeostasis in human should be proceeded.

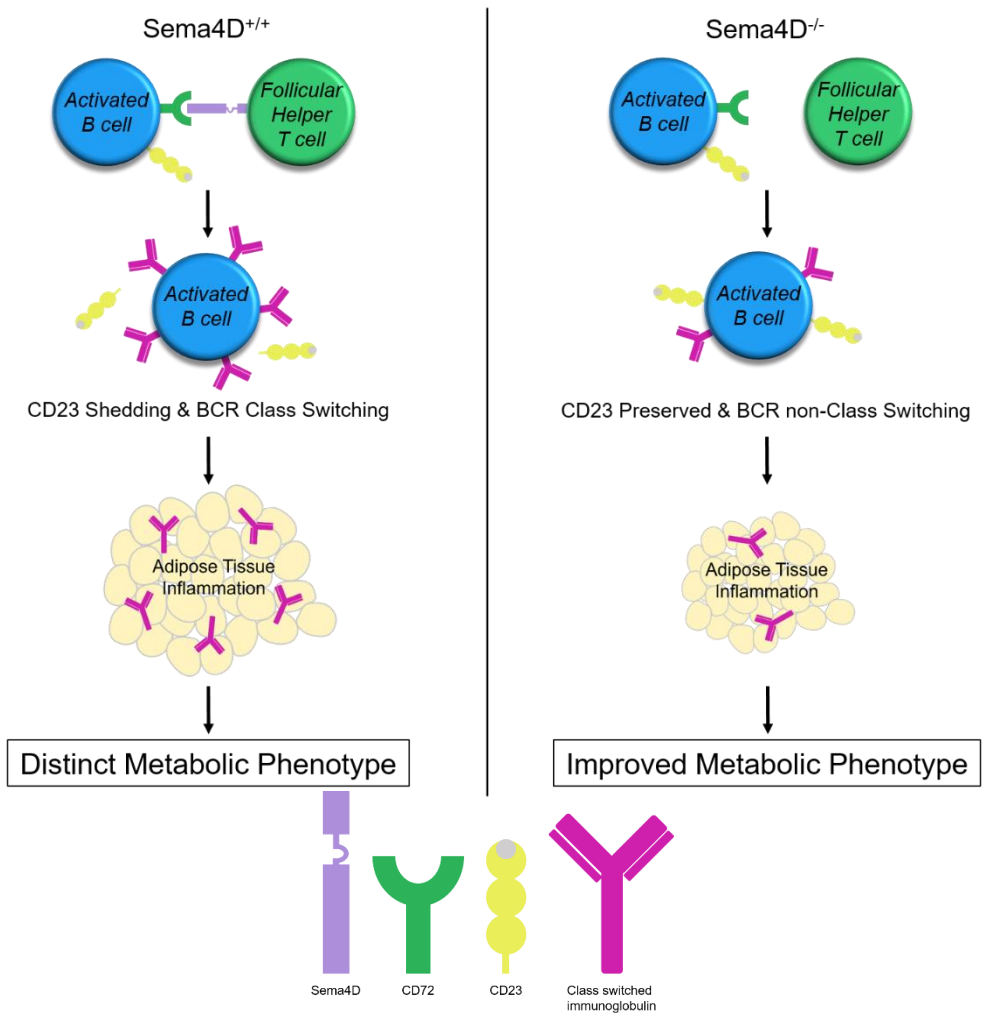

Figure 8. Metabolic effects of Semaphorin 4D.

Collectively, our results demonstrated that the immature B cell development in Sema4D KO mice inhibited class switching and systemic inflammation, which resulted in reduced adipose tissue inflammation and improved metabolic phenotype (Fig. 8). Our data suggests the importance of modulating B cell for treating obesity, glucose intolerance and insulin resistance. Also, inactivation or suppression of Sema4D could be one of the candidates for alleviating glucose dysfunction.

Conclusions

- High fat diet increases Sema4D expression in spleen
- HFD Sema4D KO mice show decreased by weight resulted from reduced fat mass
- HFD Sema4D KO mice have improved glucose intolerance and insulin resistance
- B cell development and differentiation in HFD Sema4D KO mice are reduced
- Production of pathogenic immunoglobulin IgG2c is decreased since class switching is reduced in HFD Sema4D KO
- IgG2c level in adipose tissue is decreased and infiltration of macrophages is reduced
- Reduced pathogenic response in adipose tissue decreases adipose tissue inflammation and improve glucose dysfunction

References

1. Kumanogoh, A. & Kikutani, H. Biological functions and signaling of a transmembrane semaphorin, CD100/Sema4D. *Cell. Mol. Life Sci*. **61**, 292-300 (2004)

2. Wu, H. J. & Bondada, S. Positive and negative roles of CD72 in B cell function. *Immunol. Res.* **25**, 155-66 (2002)

3. Shi, W., Kumanogoh, A., Watanabe, C., Uchida, J., Wang, X., Yasui, T., Yukawa, K., Ikawa, M., Okabe, M., Parnes, J. R., Yoshida, K. & Kikutani, H. The class IV semaphorin CD100 plays nonredundant roles in the immune system: defective B and T cell activation in CD100-deficient mice. *Immunity* **13**, 633-42 (2000)

4. Yang, Y. H., Zhou, H., Binmadi, N. O., Proia, P. & Basile, J. R. Plexin-B1 activates NF-κB and IL-8 to promote a pro-angiogenic response in endothelial cells. *PLoS One* **6**, e25826 (2011)

5. Zhang, C., Xiao, C., Dang, E., Cao, J., Zhu, Z., Fu, M., Yao, X., Liu, Y., Jin, B., Wang, G. & Li, W. CD100-Plexin-B2 promotes the inflammation in psoriasis by activating NF-κB and the inflammation in keratinocytes. *J. Invest. Dermatol.* **138**, 375-383 (2018)

6. Shen, S., Ke, Y., Dang, E., Fang, H., Chang, Y., Zhang, J., Zhu, Z.,

Shao, S., Qiao, P., Zhang, T., Qiao, H. & Wang, G. Semaphorin 4D from CD15+ granulocytes via ADAM10-induced cleavage contributes to antibody production in bullous pemphigoid. *J. Invest. Dermatol.* **138**, 588-597 (2018)

7. Gordon, J. B-cell signaling via the C-type lectins CD23 and CD72. *Immunol. Today* **15**, 411-7 (1994)

8. Winer, D. A., Winer, S., Shen, L., Wadia, P. P., Wantha, J., Paltser, G., Tsui, H., Wu, P., Davidson, M. G., Alonso, M. N., Leong, H. X., Glassford, A., Caimol, M., Kenkel, J. A., Tedder, T. F., McLaughlin, T., Miklos, D. B., Dosch, H.M. & Engleman, E. G. B cells promote insulin resistance through modulation of T cells and production of pathogenic IgG antibodies. *Nat. Med.* **17**, 610-7 (2011)

9. García-Hernández, M. H., Rodríguez-Varela, E., García-Jacobo, R. E., Hernández-De la Torre, M., Uresti-Rivera, E. E., González-Amaro, R. & Portales-Pérez, R. E. Frequency of regulatory B cells in adipose tissue and peripheral blood from individuals with overweight, obesity and normal-weight. *Obes. Res. Clin. Racti.* **12**, 513-519 (2018)

10. Shen, L. Chng, M. H. Y., Alonso, M. N., Yuan, R., Winer, D. A. & Englemen, E. G. B-1a lymphocytes attenuate insulin resistance. *Diabetes* **64**, 593-603 (2015)

11. Duan, B. & Morel, L. Role of B-1a cells in autoimmunity. *Autoimmun.*

Rev. **5**, 403-8 (2006)

12. Kumanogoh, A., Watanabe, C., Lee, I., Wang, X., Shi, W., Araki, H., Hirata, H., Iwahori, K., Uchida, J., Yasui, T., Matsumoto, M., Yoshida, K., Yakura, H., Pan, C., Parnes, J. R. & Kikutani, H. Identification of CD72 as a lymphocyte receptor for the class IV semaphoring CD100: a novel mechanism for regulating B cell signaling. *Immunity* **13**, 621-31 (2000)

13. Ota, T. Chemokin systems link obesity to insulin resistance. *Diabetes. Metab. J.* **37**, 165-72 (2013)

14. Makki, K., Froguel, P. & Wolowczuk, I. Adipose tissue in obesity-related inflammation and insulin resistance: cells, cytokines, and chemokines. *ISRN Inflamm.* **2013**, 139239 (2013)

15. Shoelson, S. E., Lee, J. & Coldfine, A. B. Inflammation and insulin resistance. *J. Clin. Invest.* **116**, 1793-801 (2006)

16. Li, P., Oh, D. Y., Bandyopadhyay, G., Lagakos, W. S., Talukdar, S., Osborn, O., Johnson, A., Chung, H., Maris, M., Ofrecio, J. M., Taguchi, S., Lu, M. & Olefsky, J. M. LTB4 promotes insulin resistance in obese mice by acting on macrophages, hepatocytes and myocytes. *Nat. Med.* **21**, 239-247 (2015)

17. Lee, Y. S., Wollam, J. & Olefsky, J. M. An integrated view of immunometabolism. *Cell* **172**, 22-40 (2018)

18. Hotamisligil, G. S. Inflammation, metaflammation and immunometabolic disorders. *Nature* **542**, 177-185 (2017)

19. Winer, D. A., Winer, S., Chng, M. H., Shen, L. & Engleman, E. G. B lymphocytes in obesity-related adipose tissue inflammation and insulin resistance. *Cell. Mol. Life Sci.* **71**, 1033-43 (2014)

20. Kumanogoh, A. & Kikutani, H. The CD100-CD72 interaction: a novel mechanism of immune regulation. *Trends. Immunol.* **22**, 670-6 (2001)

21. Maleki, K. T., Cornillet, M. & Björkström, N. K. Soluble SEMA4D/CD100: A novel immunoregulator in infectious and inflammatory disease. *Clin. Immunol.* **163**, 52-9 (2016)

22. Elhabazi, A., Delaire, S., Bensussan, A., Boumsell, L. & Bismuth, G. Biological activity of soluble CD100. I. The extracellular region of CD100 is released from the surface of T lymphocytes by regulated proteolysis. *J. Immunol.* **166**, 4341-7 (2001)

23. Wang, X., Kumanogoh, A., Watanabe, C., Shi, W., Yoshida, K. & Kikutani, H. Functional soluble CD100/Sema4D released from activated lymphocytes: possible role in normal and pathologic immune responses. *Blood* **97**, 3498-504 (2001)

24. Alto, L. T. & Terman, J. R. Semaphorins and their signaling mechanisms. *Methods. Mol. Biol.* **1493**, 1-25 (2017)

25. Frasca, D. & Blomberg, B. B. Adipose tissue inflammation induces B cell inflammation and decreases B cell function in aging. *Front. Immunol.* **8**, 1003 (2017)

26. Lyu, M., Hao, Y., Li, Y., Lyu, C., Liu, W., Li, H., Xue, F., Liu, X. & Yang, R. Upregulation of CD72 expression on $CD19^{+}CD27^{+}$ memory B cells by CD40L in primary immune thrombocytopenia. *Br. J. Haematol.* **178**, 308-318 (2017)

27. Tanigaki, K., Sacharidou, A., Peng, J., Chambliss, K. L. , Yuhanna, I. S., Ghosh, D., Ahmed, M., Szalai, A. J., Vongpatanasin, W., Mattrey, R. F., Chen, Q., Azadi, P., Lingvay, I., Botto, M., Holland, W. L., Kohler, J. K., Sirsi, S. R., Hoyt, K., Shaul, P. W. & Mineo, C. Hyposialylated IgG activates endothelial IgG receptor FcγRIIB to promote obesity-induced insulin resistance. *J. Clin. Invest.* **128**, 309-322 (2018)

28. Nakano, S., Morimoto, S., Suzuki, J., Mitsuo, A., Nakiri, Y., Katagiri, A., Nozawa, K., Amano, H., Tokano, Y., Hashimoto, H. & Takasaki, Y. Down-regulation of CD72 and increased surface IgG on B cells in patients with lupus nephritis. *Autoimmunity* **40**, 9-15 (2007)

29. Suzuki, K., Kumanogoh, A. & Kikutani, H. Semaphorins and their receptors in immune cell interactions. *Nat. Immunol.* **9**, 17-23 (2008)

30. Li, M., O'Sullivan, K. M., Jones, L. K., Lo, C., Semple, T.,

Kumanogoh, A., Kikutani, H., Holdsworth, S. R. & Kitching, R. Endogenous CD100 promotes glomerular injury and macrophage recruitment in experimental crescentic glomerulonephritis. *Immunology* **128,** 114-22 (2009)

31. Chen, G., Doumatey, A. P., Zhou, J., Lei, L., Bentley, A. R., Tekola-Ayele, F., Adebamowo, S. N., Baker, J. L., Fasanmade, O., Okafor, G., Eghan, Jr. B., Agyenim-Boateng, K., Amoah, A., Adebamowo, C., Acheampong, J., Johnson, T., Oli, J., Shriner, D., Adeyemo, A. A. & Rotimi, C. N. Genome-wide analysis identifies an African-specific variant in SEMA4D associated with body mass index. *Obesity* **25**, 794-800 (2017)

32. Hall, K. T., Boumsell, L., Schultze, J. L., Boussiotis, V. A., Dorfman, D. M., Cardoso, A. A., Bensussan A., Nadler, L. M. & Freeman, G. J. Human CD100, a novel leukocyte semaphorin that promotes B-cell aggregation and differentiation. *Proc. Natl. Acad. Sci. U. S. A.* **93**, 11780-5 (1996)

33. Liu, C., Richard, K., Wiggins, M., Zhu, X., Conrad, D. H. & Song, W. CD23 can negatively regulate B-cell receptor signaling. *Sci. Rep.* **6**, 25629 (2016)

34. Lampert, I. A., Wotherspoon, A., Van Noorden, S. & Hasserjian, R. P. High expression of CD23 in the proliferation centers of chronic lymphocytic leukemia in lymph nodes and spleen. *Hum. Pathol.* **30**,

648-54 (1999)

35. Hunot, S., Dugas, N., Faucheux, B., Hartmann, A., Tardieu, M., Debré, P., Agid, Y., Dugas, B. & Hirsch, E. C. FcεRII/CD23 Is Expressed in Parkinson's Disease and Induces, *In Vitro,* Production of Nitric Oxide and Tumor Necrosis Factor-α in Glial Cells. *J. Neurosci.* **19**, 3440-7 (1999)

36. Wang, T. T. & Ravetch, J. V. Functional diversification of IgGs through Fc glycosylation. *J. Clin. Invest.* **129**, 3492-3498 (2019)

37. Lemieux, G. A., Blumenkron, F., Yeung, N., Zhou, P., Williams, J., Grammer, A. C., Petrovich, R., Lipsky, P. E., Moss, M. L. & Werb, Z. The low affinity IgE receptor (CD23) is cleaved by the metalloproteinase ADAM10. *J. Bio. Chem.* **282**, 14836-44 (2007)

38. Ford, J. W., Kilmon, M. A., Haas, K. M., Shelburne, A. E., Chan-Li, Y. & Conrad, D. H. In vivo murin CD23 destabilization enhances CD23 shedding and IgE synthesis. *Cell. Immunol.* **243**, 107-17 (2006)

39. Dorfman, D. M. Shahsafaei, A., Nadler, L. M. & Freeman, G. J. The leukocyte semaphorin CD100 is expressed in most T-cell, but few B-cell, non-Hodgkin's lymphomas. *Am. J. Pathol.* **153**, 255-62 (1998)

40. Corominas, M. Mestre, M., Bas, J. & Buendia, E. Distinct modulation by interferon-gamma (IFN-gamma) of CD23 expression

on B and T lymphocytes of atopic subjects. *Clin. Exp. Immunol.* **112**, 276-80 (1998)

41. Shin, J. H., Lee, S. H., Kim, Y. N., Kim, I. Y., Kim, Y. J., Kyeong, D. S., Lim, H. J., Cho, S. Y., Choi, J., Wi, Y. J., Choi, J. H., Yoon, Y. S., Bae, Y. S., Seong, J. K. AHNAK deficiency promotes browning and lipolysis in mice via increased responsiveness to β-adrenergic signaling. *Sci. Rep.* **6**, 23426 (2016)

42. Shin, J. H., Kim, I. Y., Kim, Y. N., Shin, S. M., Roh, K. J., Lee, S. H., Sohn, M., Cho, S. Y., Lee, S. H., Ko, C. Y., Kim, H. S., Choi, C. S., Bae, Y. S. & Seong, J. K. Obesity resistance and enhanced insulin sensitivity in Ahnak-/- mice fed a high fat diet are related to impaired adipogenesis and increased energy expenditure. *PLoS* One **10**, e0139720 (2015)

43. Lee, T. K., Park, Y. E., Park, C. W., Kim, B., Lee, J. C., Park, J. H., Lee, H. A., Won, M. H. & Ahn, J. H. Age-dependent changes of p53 and p63 immunoreactivities in the mouse hippocampus. *Lab. Anim. Res.* **35**, 20 (2019)

44. Park, D. J., Kang, J. B., Shah, F. A. & Koh, P. O. Resveratrol modulates the Akt/GSK-3β signaling pathway in a middle cerebral artery occlusion animal model. *Lab. Anim. Res.* **35**, 18 (2019)

45. Kang, J. B., Park, D. J., Shah, M. A., Kim, M. O. & Koh, P. O. Lipopolysaccharide induces neuroglia activation and NF-κB

activation in cerebral cortex of adult mice. *Lab Anim Res.* **35**, 19 (2019)

46. Muramatsu, M., Kinoshita, K., Fagarasan, S., Yamada, S., Shinkai, Y. & Honjo, T. Class switch recombination and hypermutation require activation-induced cytidine deaminase (AID), a potential RNA editing enzyme. *Cell* **102**, 553-63 (2000)

47. Tan, Q., Tai, N., Li, Y., Pearson, J., Pennetti, S., Zhou, Z., Wong, F. S. & Wen, L. Activation-induced cytidine deaminase deficiency accelerates autoimmune diabetes in NOD mice. *JCI Insight* **3**, e95882 (2018)

국문 초록

Sema4D Knockout Mouse의

대사 표현형 연구

서울대학교 대학원
수의학과 수의생명과학전공
(발생유전학)

김 경 은

(지도교수: 성 제 경)

국문초록

Semaphorin 4D (Sema4D, CD100)는 150kDa의 크기를 가진 semaphorin의 한 종류로써, B cell 반응을 조절하는 면역 semaphorin (immune semaphorin)의 한 종류로 알려져 있다. Sema4D는 특히 T cell 표면에서 많이 발현되는데, B cell 표면에 존재하는 Sema4D의 수용체인 CD72에 결합하여 B cell 표면에서 CD23을 제거함으로써 IgE나 IgG로의 면역 글로불린 종류 변환 (immunoglobulin class switching)을 유도한다.

Sema4D는 면역 자극에 의해 그 발현이 증가하는데, 증가된 Sema4D가 B cell 반응을 촉진시킴으로써 면역 자극에 의한 체액 면역 반응(humoral immune response)을 유도하는데 있어 중요한 분자로 작용한다. 그렇기 때문에 Sema4D는 현재까지 류마티즘과 같은 자가면역 질환과 관련되어서 주로 연구가 진행되어 왔으며, 당뇨나 인슐린 저항성에 미치는 영향에 대해서는 보고된 바가 없다. 그러나, 아프리카 사람들 중 비만인 경우에 혈중 soluble Sema4D의 농도가 높다는 임상 결과가 밝혀졌으며, B cell 또한 비만에서 포도당 내성 (glucose tolerance)과 인슐린 민감도 (insulin sensitivity)에 영향을 미친다는 선행 연구들이 진행되었다.

이에 본 논문에서는 Sema4D가 비만인 경우에 B cell 반응을 통하여 포도당 항상성 (glucose homeostasis)을 조절할 것이라는 가설을 통해 비만 환경에서 Sema4D의 역할에 대해 연구를

진행하고자 하였다. 이에 따라 WT 마우스와 Sema4D KO 마우스를 이용하여 고지방식이 (high fat diet)를 먹었을 때의 Sema4D 발현 여부에 따른 대사, 생리적 변화와 염증 변화를 확인하였다.

Sema4D KO 마우스는 고지방식이를 먹은 경우 WT 마우스에 비해 몸무게의 증가가 더디고, 지방의 무게 및 크기 또한 감소되어 있음을 확인하였다. 또한, 고지방식이에 의한 포도당 불내성과 인슐린 저항성 또한 개선됨을 확인하였다. 이에 따른 이유를 찾기 위해 C/ebp-α 등과 같이 지방 합성 (adipogenesis)을 유도하거나, Hsl 등과 같은 지방산 합성을 유도하는 지질 대사 (lipid metabolism) 관련 유전자들의 발현을 살펴보았을 때 고지방식이를 먹은 Sema4D KO 마우스에서 그 발현이 낮은 것을 확인하였다.

Sema4D는 면역 자극에 의해 그 발현이 증가하는 것이 알려져 있는데, 고지방식이를 실시한 경우에도 비장에서 그 발현이 증가하는 것을 확인하였다. 또한, B cell에 국한적으로 발현되는 Sema4D의 수용체인 CD72가 Sema4D의 발현이 일어나는 비장에서 같이 발현이 되는 것을 확인하였기 때문에, 비장에서 Sema4D의 발현 유무 및 양적 차이에 따른 염증의 변화 여부를 확인하였다. 그 결과, 고지방식이를 먹은 Sema4D KO 마우스의 비장에서는 WT 마우스의 비장에 비해 염증이 줄어든 것을 확인하였으며, 이는 B cell의 분화가 더디기 때문인 것으로 확인하였다. 실제로 고지방식이를 먹은 Sema4D KO 마우스는 CD72에 의한 B cell 하위 signaling이 감소하였으며, 이에 따라 면역 글로불린 종류 변화가 일어난 면역 글로불린인 IgG2c의 생성량이 WT 마우스에 비해 적은

것을 확인하였다.

마지막으로 이러한 변화가 지방에 어떤 영향을 주는지 확인하기 위하여 지방에서의 염증을 확인하였다. 고지방식이를 먹은 Sema4D KO 마우스의 지방에서 WT 마우스에 비해 염증성 사이토카인의 양이 감소하였으며, 지방으로의 대식세포 유입 또한 감소함을 확인하였다. 그리고 지방에서 염증성이자 병원성으로 알려진 글로불린인 IgG2c의 양이 감소한 것을 확인하였다.

결과적으로, Sema4D KO 마우스는 고지방식이를 투여하였을 때, Sema4D에 의한 CD72 하위 B cell signaling이 감소하였고, 이로 인하여 B cell의 분화가 더디게 일어났다. 따라서, 전체적인 염증 반응이 감소하였고, 병원성 면역 글로불린의 생성 양 또한 감소하였다. 병원성 면역 글로불린인 IgG2c의 생성 감소로 인하여 지방에서의 IgG2c 양 또한 감소하였는데, 이에 따른 대식 세포의 유입 및 대식 작용이 감소하였다. 대식 작용은 염증을 증가시키고, 증가된 염증은 포도당 불내성과 인슐린 저항을 증가시키는데, 고지방식이를 한 Sema4D KO 마우스에서는 이러한 대식 작용이 WT 마우스에 비해 감소되어 있었다. 이로 인해 지방에서의 염증이 감소하였고, 포도당 불내성과 인슐린 저항성 및 지방과 체중 증가에 있어서 개선되는 효과를 나타내었다.

주요 단어: Semaphorin 4D, 비만, adipose tissue inflammation, B 림프구, 인슐린 저항성, 마우스

학번: 2018-22461